Guiding center atoms: Three-body recombination in a strongly magnetized plasma

Michael E. Glinsky and Thomas M. O'Neil
University of California at San Diego, La Jolla, California 92093

(Received 10 August 1990; accepted 29 January 1991)

The three-body recombination rate is calculated for an ion introduced into a magnetically confined, weakly correlated, and cryogenic pure electron plasma. The plasma is strongly magnetized in the sense that the cyclotron radius for an electron $r_{ce} = \sqrt{k_B T_e/m_e}/\Omega_{ce}$ is small compared to the classical distance of closest approach $b = e^2/k_B T_e$, where T_e is the electron temperature and $\Omega_{ce} = eB/m_e c$ is the electron cyclotron frequency. Since the recombination rate is controlled by a kinetic bottleneck a few $k_B T_e$ below ionization, the rate may be determined by considering only the initial cascade through states of electron-ion pairs with separation of order b. These pairs may be described as guiding center atoms since the dynamics is classical and treatable with the guiding center drift approximation. In this paper, an ensemble of plasmas characterized by guiding center electrons and stationary ions is described with the BBGKY hierarchy. Under the assumption of weak electron correlation, the hierarchy is reduced to a master equation. Insight to the physics of the recombination process is obtained from the variational theory of reaction rates and from an approximate Fokker–Planck analysis. The master equation is solved numerically using a Monte Carlo simulation, and the recombination rate is determined to be $0.070(10) n_e^2 v_e b^5$ per ion, where n_e is the electron density and $v_e = \sqrt{k_B T_e/m_e}$ is the thermal velocity. Also determined by the numerical simulation is the transient evolution of the distribution function from a depleted potential well about the ion to its steady state.

I. INTRODUCTION

Recent experiments have produced magnetically confined pure electron plasmas in the cryogenic temperature range.[1] The plasmas are strongly magnetized in the sense that $r_{ce} \ll b$, where $r_{ce} = v_e/\Omega_{ce}$ is the electron cyclotron radius and $b = e^2/k_B T_e$ is the classical distance of closest approach. Here $v_e = \sqrt{k_B T_e/m_e}$ is the electron thermal speed and $\Omega_{ce} = eB/m_e c$ is the electron cyclotron frequency.

In this paper, we discuss the three-body recombination process[2] that occurs when an ion is introduced into one of these plasmas. Three-body recombination dominates since the rate for this process is very large at low temperature (i.e., $R_3 \sim T_e^{-9/2}$). To understand this scaling, note that the important energy scale in determining the rate is $k_B T_e$ and that this energy corresponds to an electron-ion separation of $b = e^2/k_B T_e$. The frequency of electron–ion collisions characterized by an impact parameter in this range is $n_e b^2 v_e$, where n_e is the electron density, and the probability that another electron is close enough to carry off energy $k_B T_e$ is of order $n_e b^3$. The three-body rate is given by the product $R_3 \sim (n_e b^2 v_e)(n_e b^3)$, and this scales as $T_e^{-9/2}$. In this discussion and in the paper as a whole, we assume that the plasma density is low enough that $n_e b^3 \ll 1$; such a plasma is said to be weakly correlated. One can easily check that radiative recombination, where a photon carries away the binding energy, is much slower than three-body recombination in the cryogenic temperature range considered here.[3,4]

The antimatter analog of the electron–ion three-body recombination process is a possible way of producing antihydrogen[3] for use in gravitational and spectroscopic studies.[5] Positron plasmas have already been produced,[6] and antiprotons have been trapped and cooled to less than 0.1 eV.[7] A logical next step is to introduce antiprotons into a positron plasma (of the same character as the cryogenic strongly magnetized electron plasma) so that the antiprotons and positrons recombine. The recombination rate is a design parameter for such experiments, and that in part motivates these theoretical studies.

For the case of zero magnetic field, the three-body recombination rate has been calculated previously.[8–10] However, when a strong magnetic field is present, a constraint is imposed on the electron dynamics (the electrons cannot move freely across the field), and the rate is reduced by an order of magnitude. The previous rate obtained for $B = 0$ is $R_3(B = 0) = 0.76(4) n_e^2 b^5 v_e$ and the strong field rate obtained here is $R_3(B = \infty) = 0.070(10) n_e^2 b^5 v_e$.

As we shall discuss below, the rate is controlled by a kinetic bottleneck[10] at a binding energy of a few $k_B T_e$ below the ionization energy. The dynamics in this range is classical, since $k_B T_e$ is much smaller (four orders of magnitude smaller) than the Rydberg energy. Also, the electron dynamics may be treated by guiding center drift theory,[11,12] since the cyclotron radius is much smaller than the scale length on which the interaction potential varies (i.e., $r_{ce} \ll b$). Equivalently, the cyclotron frequency is much larger than the next largest dynamical frequency (i.e., $\Omega_{ce} \gg v_e/b$). This implies that the high-frequency cyclotron motion may be averaged out and the number of degrees of freedom correspondingly reduced; the center of the cyclotron orbit (guiding center) moves according to guiding center drift theory.

In the energy range of the bottleneck, a bound electron–

 0899-8221/91/051279-15$02.00

ion pair from a novel atom, which we call a guiding center atom. The electron guiding center oscillates back and forth along a field line in the Coulomb well of the ion and more slowly $\mathbf{E}\times\mathbf{B}$ drifts around the ion (see Fig. 1). The frequency of oscillation back and forth along a field line is of order $\omega_z \sim \sqrt{e^2/m_e b^3} \sim v_e/b$, and the frequency of the $\mathbf{E}\times\mathbf{B}$ drift motion is of order $\omega_{\mathbf{E}\times\mathbf{B}} \sim ec/Bb^3$. One can see that a consequence of the ordering $r_{ce} \ll b$ is the ordering $\omega_z \gg \omega_{\mathbf{E}\times\mathbf{B}}$.

In this discussion and in the paper as a whole the ion is treated as stationary. This approximation makes sense when the electron motion is rapid compared to the ion motion. For example, we require that $v_e \gg v_{i\|}$, where $v_{i\|}$ is the characteristic ion velocity parallel to the magnetic field. The requirements on the transverse motion are most easily stated as the frequency ordering: $\omega_{\mathbf{E}\times\mathbf{B}} \gg v_{i\perp}/b, \Omega_{ci}$, where $v_{i\perp}$ is the characteristic ion velocity transverse to the field and $\Omega_{ci} = eB/m_i c$ is the ion cyclotron frequency.

With these orderings in mind, we develop a model based on guiding center electrons and stationary ions. Consider an ensemble of weakly correlated and guiding center electron plasmas with a single stationary ion located deep within the plasma at the origin of coordinates. A long way from the ion, the plasma is assumed to be in thermal equilibrium at density n_e and temperature T_e. The ion produces a Coulomb potential well, and collisional interactions allow an electron to fall into the well, that is, to become bound to the ion. Between collisions with other electrons the electron–ion pair from a guiding center atom. As the atom undergoes a sequence of collisions, the atom may be reionized or it may cascade in energy to very deep binding. Note that in some of these collisions the incident electron may replace the originally bound electron. At a very deep level of binding there is a sink; any electron that reaches this level is formally removed from the vicinity of the ion and returned to the background plasma. The recombination rate is then the steady state flux of electrons into the sink. We will find that the value of this rate does not depend on the exact location of the sink, provided the sink is below the kinetic bottleneck.

In Sec. II, the BBGKY hierarchy for the ensemble is discussed.[13] The equations of the hierarchy contain two small parameters, $(r_{ce}/b) \ll 1$ and $n_e b^3 \ll 1$, and we analyze the equations to lowest nontrivial order in these parameters. The smallness of r_{ce}/b implies that the $\mathbf{E}\times\mathbf{B}$ drift motion that occurs during a collision is negligible; recall that $r_{ce}/b \ll 1$ implies that $v_e/b \gg \omega_{\mathbf{E}\times\mathbf{B}}$. Because the most important collisions are close collisions (particle separation $\sim b$) and because the plasma is low density (i.e., $n_e b^3 \ll 1$), the hierarchy can be truncated by neglecting three-electron collisions. The first and second equations of the hierarchy then form a closed set. These two equations are formally reduced to a master equation; but the transition rates in the master equation (for steps in the recombination cascade) are not known analytically. In general, these rates depend on the complicated collision dynamics of two electrons in the force field of an ion. Consequently, a rigorous analytic solution of the master equation is not possible. However, two approximate treatments of the hierarchy equations yield important physical insights into the recombination process, so we discuss these treatments before going on to a proper numerical solution of the master equation.

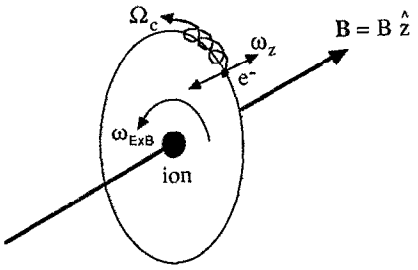

FIG. 1. Drawing of guiding center atom. In order of descending frequency, the electron executes cyclotron motion, oscillates back and forth along a field line in the Coulomb well of the ion, and $\mathbf{E}\times\mathbf{B}$ drifts around the ion.

The first of these treatments is discussed in Sec. III, where the collisional dynamics is solved perturbatively and the hierarchy equations are reduced to a Fokker–Planck equation.[14] This approximation makes sense when the collisional cascade toward deeper binding takes place through many small and random steps. Each collision is assumed to produce a step in binding energy that is small compared to the energy scale on which the electron energy distribution varies. The step in energy is in fact small and the dynamics treatable perturbatively for collisions characterized by sufficiently large impact parameter. Unfortunately, it is clear from the Fokker–Planck coefficients that small impact parameter collisions make an important contribution, so the analysis in Sec. III is not the whole story. However, the analysis does provide an important insight. Consider a bound electron–ion pair and a second electron that is incident on the pair. Suppose that the oscillation period of the bound electron is short compared to the duration of the collision. In this case, the oscillation is characterized by a good adiabatic invariant, and the collision changes the binding energy only by an exponentially small amount. We refer to the impact parameter beyond which the energy perturbation is exponentially small as the adiabatic cutoff.

In Sec. IV, a variational theory of the recombination rate is presented.[15] The underlying assumption for this treatment is the opposite of that for the Fokker–Planck treatment; the distribution function is assumed to vary on an energy scale that is small compared to a typical step size. In particular, the two-electron distribution $f_2(1,2)$ is taken to be of the thermal equilibrium form if electron 1 is bound less deeply than some energy E, and is taken to be zero if electron 1 is bound more deeply. Electron 2 is assumed to be a free electron that is incident on bound electron 1. The interaction of electron 2 with electron 1 produces a flux of electron 1 toward deeper binding: the one-way thermal equilibrium flux through the energy surface $E(1) = E$. This flux is shown to scale as the product of the Boltzmann factor $\exp(\varepsilon)$ and the phase space factor ε^{-4}, where $\varepsilon = E/k_B T_e$ and binding energy is taken to be positive toward deeper binding. The flux $[\sim \exp(\varepsilon)/\varepsilon^4]$ has a strong minimum at $\varepsilon = 4$, and this minimum is the kinetic bottleneck. The variational theory takes the recombination rate to be the value of

this one way flux at the bottleneck.

From the existence of the bottleneck, we may deduce the following picture. As atoms are formed and cascade to deeper binding, only a small fraction get through the bottleneck; the rest are re-ionized. If an atom makes it through the bottleneck, it continues to ever deeper binding with only a small probability of being re-ionized. Well above the bottleneck the distribution is very nearly of the thermal equilibrium form, and well below the bottleneck the distribution is depleted relative to thermal equilibrium.

This picture motivates the basic assumption of the variational theory, namely, that the distribution is of the thermal equilibrium form for $E(1) < E$ and is zero for $E(1) > E$. Of course, the assumption is an idealization; the actual distribution does not drop off discontinuously, but rather falls off gradually over a finite range in energy. There will now be fewer atoms with $E(1) < E$ which can change to a state with $E(1) > E$ over the course of a collision.. In addition, the atoms bound with $E(1) > E$ will be able to change to a state with $E(1) < E$ leading to a return flux. This is particularly a problem for large impact parameter collisions, where the step size is small. The flux associated with these collisions is diffusive in nature and is greatly overestimated by the one way flux. Another problem is the fact that the one-way flux is instantaneous. If an atom recrosses the surface $E(1) = E$ during the course of a collision, it will be counted too many times by the one-way flux. Large impact parameter collisions will again contribute most to such recrossings. To rectify these problems, the variational theory imposes a cutoff at large impact parameter. This cutoff is introduced in an *ad hoc* fashion, and the value of the cutoff is not determined within the context of the theory. Crude arguments from the Fokker–Planck analysis suggest that the cutoff should be of order b. Also, the actual one-electron distribution is not simply a function of energy, as is assumed in the variational theory, but also depends on the separation between the field line through the ion and the field line through the bound electron. One expects such a dependence in the strong magnetic field case, because the electrons are not free to move across the field.

Because neither the Fokker–Planck treatment nor the variational treatment is entirely satisfactory, the cascade dynamics is followed numerically in Sec. V. Guiding center atoms are formed and then followed through a sequence of collisions, with the incident electron picked at random from a Maxwellian distribution. This procedure can be justified formally as a Monte Carlo solution of the master equation.[16] The solution verifies the existence of the bottleneck and determines the recombination rate. In addition, the time-dependent behavior of the distribution function is obtained. The result is a quantitative understanding of how the initially depleted potential well is filled to the steady-state condition.

II. BASIC EQUATIONS

In this section, we develop the BBGKY hierarchy[13] for the ensemble of guiding center plasmas described in the Introduction. Anticipating that the important energy scale is $k_B T_e$, we scale the lengths by $b = e^2/k_B T_e$, velocities by $v_e = \sqrt{k_B T_e/m_e}$, and time by b/v_e. In terms of scaled variables, Liouville's equation for the ensemble is given by[13,14]

$$\frac{\partial D_N}{\partial t} + \sum_{j=1}^{N} v_j \frac{\partial D_N}{\partial z_j} - \sum_{\substack{j=1 \\ i=0}}^{N} \frac{\partial \phi_{ji}}{\partial z_j} \frac{\partial D_N}{\partial v_j} + \left(\frac{r_{ce}}{b}\right) \sum_{\substack{j=1 \\ i=0}}^{N} \hat{z} \times \nabla_j \phi_{ji} \cdot \nabla_j D_N = 0, \tag{1}$$

where $D_N(\mathbf{r}_1, v_1, \cdots, \mathbf{r}_N, v_N, t)$ is the N-electron distribution normalized to unity (i.e., $\int d\mathbf{r}_1\, dv_1 \cdots d\mathbf{r}_N\, dv_N\, D_N = 1$). We have used Cartesian coordinates with a uniform magnetic field $\mathbf{B} = B\hat{z}$ and the velocity in the $\hat{z}$ direction. Particle $i = 0$ is the ion (i.e., $\phi_{j0} = -1/|\mathbf{r}_j|$ for $j = 1,...,N$) and the remaining particles are electrons (i.e., $\phi_{ij} = 1/|\mathbf{r}_i - \mathbf{r}_j|$ for $i, j = 1,...,N$).

The s-electron function is defined as[13]

$$f_s = \frac{V^s}{b^{3s}} \int d\mathbf{r}_{s+1}\, dv_{s+1} \cdots d\mathbf{r}_N\, dv_N\, D_N, \tag{2}$$

where V is the plasma volume. To obtain the first equation of the hierarchy, we integrate Eq. (1) over the variables for the last $(N-1)$ electrons [i.e., take $s = 1$ in Eq. (2)] and obtain

$$\frac{\partial f_1}{\partial t}(1) + v_1 \frac{\partial f_1}{\partial z_1} - \frac{\partial \phi_{10}}{\partial z_1} \frac{\partial f_1}{\partial v_1} + \left(\frac{r_{ce}}{b}\right) \hat{z} \times \nabla_1 \phi_{10} \cdot \nabla_1 f_1(1) = n_e b^3 \int d\mathbf{r}_2\, dv_2 \times \left[\frac{\partial \phi_{12}}{\partial z_1} \cdot \frac{\partial}{\partial v_1} - \left(\frac{r_{ce}}{b}\right) \hat{z} \times \nabla_1 \phi_{12} \cdot \nabla_1\right] f_2(1,2), \tag{3}$$

where we have set $(N-1)/V \cong n_e$. Integrating Eq. (1) over the variables for the last $(N-2)$ electron yields the second equation

$$\frac{\partial f_2}{\partial t}(1,2) + \sum_{j=1}^{2} \left[v_j \frac{\partial}{\partial z_j} - \frac{\partial \phi_{j0}}{\partial z_j} \frac{\partial}{\partial v_j} + \left(\frac{r_{ce}}{b}\right) \hat{z} \times \nabla_j \phi_{j0} \cdot \nabla_j\right] f_2(1,2) + \left[-\frac{\partial \phi_{12}}{\partial z_1}\left(\frac{\partial}{\partial v_1} - \frac{\partial}{\partial v_2}\right) + \left(\frac{r_{ce}}{b}\right) \hat{z} \times \nabla_1 \phi_{12} \cdot (\nabla_1 - \nabla_2)\right] f_2(1,2) = n_e b^3 \int d\mathbf{r}_3\, dv_3 \sum_{j=1}^{2} \left[\frac{\partial \phi_{j3}}{\partial z_j} \frac{\partial}{\partial v_j} - \left(\frac{r_{ce}}{b}\right) \hat{z} \times \nabla_j \phi_{j3} \cdot \nabla_j\right] f_3(1,2,3). \tag{4}$$

These equations involve two small parameters, $(r_{ce}/b) \ll 1$ and $n_e b^3 \ll 1$, and we analyze the equations to lowest nontrivial order in these parameters. First, let us note that all terms of order (r_{ce}/b) may be dropped. All such terms in Eq. (4) and in the bracket on the right-hand side of Eq. (3) are compared to a term of order unity and consequently are negligible. This argument does not apply to the fourth term on the left-hand side of Eq. (3). We will find that the second and third term on the left combine to be of order $n_e b^3 \ll 1$, and is not necessarily the case that r_{ce}/b is smaller than

$n_e b^3$. On the other hand, symmetry implies that the one-electron distribution is of the form $f_1(1) = f_1(z_1,\rho_1,v_1,t)$, where $\rho_1^2 = x_1^2 + y_1^2$, so the fourth term vanishes identically.

Physically, we are neglecting the $\mathbf{E}\times\mathbf{B}$ drift motion that occurs during a collision; recall that $r_{ce}/b \ll 1$ implies that $v_e/b \gg \omega_{E\times B}$. For an electron bound to the ion, we are not neglecting the $\mathbf{E}\times\mathbf{B}$ drift motion that occurs between collisions. This motion is described by the fourth term on the left-hand side of Eq. (3), and this term vanishes by symmetry.

On the right-hand side of Eq. (3), $f_2(1,2)$ is multiplied by $n_e b^3$, so a zeroth-order solution may be used for $f_2(1,2)$. Thus, the term on the right-hand side of Eq. (4) may be dropped, and a closed set of equations involving only $f_1(1)$ and $f_2(1,2)$ is obtained, that is, the hierarchy of equations is truncated.

This truncation procedure is different from that typically followed in plasma kinetic theory.[17] Focusing on the long-range nature of the Coulomb interaction, one typically rewrites $f_2(1,2)$ and $f_3(1,2,3)$ in terms of a Mayer cluster expansion and truncates the hierarchy through an expansion in the weakness of correlations, or equivalently, an expansion in the weakness of the long-range interactions. Here, we are interested in close collisions (impact parameter $\sim b$) and for such collisions the interaction strength is not weak (i.e., $e^2/b = k_B T_e$). We focus the analysis on these close collisions and neglect the effect of long-range interactions; one may imagine that the functions $\phi_{ij}(\mathbf{r}_i - \mathbf{r}_j)$ are cut off for particle separation somewhat larger than b. The system is then similar to a low density neutral gas, that is, a gas for which the force range is small compared to the interparticle spacing (i.e., $n_e b^3 \ll 1$), and the truncation procedure used is the same as that for such a gas.[13]

The kind of effect that is lost in this procedure is Debye shielding.[17] However, this is unimportant for the small particle separations of interest here; the shielded interaction is nearly identical to the bare interaction for particle separation of order b, since b is much smaller than the Debye length. Note that the inequality $n_e b^3 \ll 1$ implies the inequality $b \ll \lambda_D$. Also lost in this procedure are the relatively low frequency fluctuations (i.e., $\omega \sim \omega_p = v_e/\lambda_D$) associated with the long range interactions, but one expects these to be unimportant because of the adiabatic invariant associated with the bounce motion of a bound electron (i.e., $\omega_z \gg v_e/\lambda_D$).

In rewriting Eqs. (3) and (4), it is useful to change variables from v_j to $\varepsilon_j = -[v_j^2/2 + \phi_{j0}(z_j,\rho_j)]$, where $j = 1,2$. The new variable, ε_j, is the binding energy of electron j scaled by $k_B T_e$; the minus sign is introduced so that binding energy increases positively toward deeper binding. By making this change of variables, dropping the $\mathbf{E}\times\mathbf{B}$ drift terms, and dropping the three-electron interaction term, Eqs. (3) and (4) take the simple form

$$\frac{\partial f_1(1)}{\partial t} + v_1 \frac{\partial f_1(1)}{\partial z_1} = -n_e b^3 \int d\mathbf{r}_2\, dv_2 \frac{\partial \phi_{12}}{\partial z_1} v_1 \frac{\partial f_2(1,2)}{\partial \varepsilon_1}, \tag{5}$$

$$\frac{\partial f_2(1,2)}{\partial t} + \left(v_1 \frac{\partial}{\partial z_1} + v_2 \frac{\partial}{\partial z_2} \right) f_2(1,2) + \frac{\partial \phi_{12}}{\partial z_1} \left(v_1 \frac{\partial}{\partial \varepsilon_1} - v_2 \frac{\partial}{\partial \varepsilon_2} \right) f_2(1,2) = 0, \tag{6}$$

where $\partial/\partial z_j$ is to be carried out at constant ε_j.

Since the right-hand side of Eq. (5) is of order $n_e b^3 \ll 1$, the left-hand side of the equation dominates the initial evolution of $f_1(1)$. During this evolution, $f_1(1)$ becomes nearly independent of z_1, that is, it evolves to the form

$$f_1(1) = \bar{f}_1(\rho_1,\varepsilon_1,t) + f_1'(z_1,\rho_1,\varepsilon_1,t), \tag{7}$$

where $f_1'/\bar{f}_1 \sim n_e b^3 \ll 1$. On a longer time scale (the collisional time scale), $\bar{f}_1(\rho_1,\varepsilon_1,t)$ evolves in a manner determined by the right-hand side. Substituting Eq. (7) into Eq. (5) and retaining terms of order $n_e b^3$ yields the result

$$\frac{\partial \bar{f}_1}{\partial t} + v_1 \frac{\partial f_1'}{\partial z_1} = -n_e b^3 \int d\mathbf{r}_2\, dv_2 \frac{\partial \phi_{12}}{\partial z_1} v_1 \frac{\partial f_2(1,2)}{\partial \varepsilon_1}. \tag{8}$$

For the energy regime $\varepsilon_1 > 0$ (the regime where electron 1 is bound to the ion), we operate on both sides of the equation with the integral $\oint_{\varepsilon_1} dz_1/v_1(z_1,\rho_1,\varepsilon_1)$. Since the integral is carried out over a closed loop in phase space, the second term on the left is projected out and the equation reduced to the form

$$\tau_1 \frac{\partial \bar{f}_1}{\partial t}(\rho_1,\varepsilon_1) = -\frac{\partial}{\partial \varepsilon_1} n_e b^3 \oint_{\varepsilon_1} dz_1 \int d\mathbf{r}_2\, dv_2 \frac{\partial \phi_{12}}{\partial z_1} f_2(1,2), \tag{9}$$

where $\tau_1 = \tau(\rho_1,\varepsilon_1)$ is the period of the oscillatory motion for electron 1.

For the energy regime $\varepsilon_1 < 0$, we don't have to solve for $\bar{f}_1$. This regime corresponds to unbound electrons that stream in from infinity and back out to infinity. By hypothesis the plasma is in equilibrium a long way from the ion, so $\bar{f}_1(\varepsilon_1,\rho_1)$ must be of the thermal equilibrium form

$$\bar{f}_1(\rho_1,\varepsilon_1) = f_{th}(\varepsilon_1) \equiv e^{\varepsilon_1}/\sqrt{2\pi}. \tag{10}$$

There is one aspect of this distribution that can be confusing. The spatial dependence is of the form $\exp[\phi_{10}(z_1,\rho_1)]$, which is what one expects for a bare ion. However, some of the ions have a bound electron, and the electron screens out the ion potential ϕ_{10} (this is short range screening, not long range Debye screening). The reader may ask why such screening is not manifest in Eq. (10). The point is that only a small fraction of the ions have a bound electron; we will verify *a posteriori* that the fraction is of order $n_e b^3 \ll 1$. Note in this regard that an electron that reaches the sink is declared to be recombined and is removed from the vicinity of the ion. The reason that only a small fraction of the ions have a bound electron is that the cascade time is smaller than the recombination time by a factor $n_e b^3 \ll 1$.

There is no small parameter in Eq. (6), so all of the terms are of order unity (or of order v_e/b when written in unscaled variables). In accord with Bogoliubov's ideas,[13] one expects $f_2(1,2)$ to relax to become a functional of $f_1(1)$ on the time scale v_e/b. In the remainder of this section, we will use this functional dependence to rewrite Eq. (9) first as a Boltzmann-like equation and then as a master equation. This latter equation will be used as the framework for the numerical solution developed in Sec. V.

After the relaxation has occurred, the term $\partial f_2(1,2)/\partial t$

in Eq. (6) is nonzero only because $f_1(1)$ varies in time. However, this latter variation is of order $n_e b^3$, and hence is negligible to zeroth order in $n_e b^3$. Dropping $\partial f_2(1,2)/\partial t$ and operating on the remaining terms with $\oint_{\varepsilon_1} dz_1/v_1 \int d\mathbf{r}_2\, dv_2$ yields the result

$$\oint_{\varepsilon_1} \frac{dz_1}{v_1} \int d\mathbf{r}_2\, dv_2 \left(v_1 \frac{\partial}{\partial z_1} + v_2 \frac{\partial}{\partial z_2} \right) f_2(1,2)$$
$$= -\oint_{\varepsilon_1} \frac{dz_1}{v_1} \int d\mathbf{r}_2\, dv_2 \frac{\partial \phi_{12}}{\partial z_1}$$
$$\times \left(v_1 \frac{\partial}{\partial \varepsilon_1} - v_2 \frac{\partial}{\partial \varepsilon_2} \right) f_2(1,2), \tag{11}$$

where particle 1 is assumed to be bound (i.e., $\varepsilon_1 > 0$). The first term in the bracket on the left-hand side vanishes because the integral $\oint_{\varepsilon_1} dz_1\, \partial f_2/\partial z_1$ is around a closed loop in phase space, and the second term in the bracket on the right-hand side vanishes because of the integration over v_2. Carrying out the integral over z_2 on the left-hand side then yields the result

$$\oint_{\varepsilon_1} \frac{dz_1}{v_1} \int d\mathbf{r}_{2\perp}\, dv_2\, v_2 \left[f_2(z_2 = +\infty) - f_2(z_2 = -\infty) \right]$$
$$= -\frac{\partial}{\partial \varepsilon_1} \oint_{\varepsilon_1} dz_1 \int d\mathbf{r}_2\, dv_2 \frac{\partial \phi_{12}}{\partial z_1} f_2(1,2), \tag{12}$$

where the right-hand side is the same as the right-hand side of Eq. (9) (except for a factor of $n_e b^3$).

In evaluating the bracket on the left-hand side, we first consider the region of phase space where $v_2 > 0$. The distribution $f_2(z_2 = -\infty)$ describes a bound electron 1 (recall that $\varepsilon_1 > 0$) and an incident electron 2 before the collision has occurred. In this region of phase space, the electrons are uncorrelated, so we may set $f_2(z_2 = -\infty) = \bar{f}_1(\rho_1,\varepsilon_1) \times \bar{f}_1(\rho_2,\varepsilon_2)$. The distribution $f_2(z_2 = +\infty)$ is evaluated in a region where electron 2 is coming from the collision, so electrons 1 and 2 are correlated. To evaluate the distribution in this region, we first note that Eq. (6) implies that $f_2(1,2) = f_2(1',2')$, where $(1',2')$ is a phase space point that evolves into $(1,2)$. Thus, we may set $f_2(z_2 = \infty) = \bar{f}_1(\rho_1,\varepsilon_1') \times \bar{f}_1(\rho_2,\varepsilon_2')$, where $(\rho_1,\varepsilon_1',\rho_2,\varepsilon_2')$ evolves into $(\rho_1,\varepsilon_1,\rho_2,\varepsilon_2)$ during the collision. Again we have used the fact that the electrons are uncorrelated before the collision. Substituting these expressions into Eq. (12) and then substituting for the right-hand side of Eq. (9) yields the Boltzmann-like equation[13]

$$\frac{\partial \bar{f}_1}{\partial t}(\rho_1,\varepsilon_1)$$
$$= n_e b^3 \frac{1}{\tau_1} \oint_{\varepsilon_1} \frac{dz_1}{v_1} \int d\mathbf{r}_{2\perp}\, dv_2\, |v_2|$$
$$\times \left[\bar{f}_1(\rho_1,\varepsilon_1') \bar{f}_1(\rho_2,\varepsilon_2') - \bar{f}_1(\rho_1,\varepsilon_1) \bar{f}_1(\rho_2,\varepsilon_2) \right], \tag{13}$$

where the absolute value sign on v_2 is needed to make the integrand valid for $v_2 < 0$ as well as $v_2 > 0$.

To obtain a master equation, we first rewrite Eq. (13) in the form

$$\frac{\partial \bar{f}_1}{\partial t} = n_e b^3 \frac{1}{\tau_1} \oint_{\varepsilon_1} \frac{dz_1}{v_1} \int d\mathbf{r}_{2\perp}\, dv_2\, |v_2|\, f_{\rm th}(\varepsilon_1) f_{\rm th}(\varepsilon_2)$$
$$\times \left(\frac{\bar{f}_1(\rho_1,\varepsilon_1') \bar{f}_1(\rho_2,\varepsilon_2')}{f_{\rm th}(\varepsilon_1') f_{\rm th}(\varepsilon_2')} - \frac{\bar{f}_1(\rho_1,\varepsilon_1) \bar{f}_1(\rho_2,\varepsilon_2)}{f_{\rm th}(\varepsilon_1) f_{\rm th}(\varepsilon_2)} \right), \tag{14}$$

where $f_{\rm th}(\varepsilon_1)$ is the thermal distribution given in Eq. (10) and we have used conservation of energy ($\varepsilon_1' + \varepsilon_2' = \varepsilon_1 + \varepsilon_2$). In the post-collision state, particle 2 is free (i.e., $\varepsilon_2 < 0$) so $\bar{f}_1(\rho_2,\varepsilon_2) = f_{\rm th}(\varepsilon_2)$. In the pre-collision state particle 1, particle 2, or both particles 1 and 2 are free. We choose the particle with largest binding energy, and denote its variables by (ρ',ε'), that is, we define $\varepsilon' = \max(\varepsilon_1',\varepsilon_2')$ and let ρ' be the corresponding ρ_1 or ρ_2. The other particle is guaranteed to be free and to have a thermal distribution. Thus, Eq. (14) reduces to the form

$$\frac{\partial \bar{f}_1}{\partial t}(\rho_1,\varepsilon_1) = f_{\rm th}(\varepsilon_1) n_e b^3 \frac{1}{\tau_1} \oint_{\varepsilon_1} \frac{dz_1}{v_1} \int d\mathbf{r}_{2\perp}\, dv_2\, |v_2|$$
$$\times f_{\rm th}(\varepsilon_2) \left(\frac{\bar{f}_1(\rho',\varepsilon')}{f_{\rm th}(\varepsilon')} - \frac{\bar{f}_1(\rho_1,\varepsilon_1)}{f_{\rm th}(\varepsilon_1)} \right). \tag{15}$$

Let us define the forward transition rate

$$k_+(\rho_1,\varepsilon_1|\bar{\rho},\bar{\varepsilon})$$
$$= n_e b^3 \frac{1}{\tau_1} \oint_{\varepsilon_1} \frac{dz_1}{v_1} \int \rho_2\, d\rho_2\, d\theta_2\, dv_2\, |v_2|\, f_{\rm th}(\varepsilon_2)$$
$$\times \delta[\bar{\varepsilon} - \varepsilon_+(z_1,\rho_1,\varepsilon_1,\rho_2,\theta_2,\varepsilon_2)]$$
$$\times \delta[\bar{\rho} - \rho_+(z_1,\rho_1,\varepsilon_1,\rho_2,\theta_2,\varepsilon_2)], \tag{16a}$$

where the plus indicates evolution forward in time from an initial state characterized by $(z_1,\rho_1,\varepsilon_1,\rho_2,\theta_2,\varepsilon_2)$. Here, electron 1 is initially bound ($\varepsilon_1 > 0$) and electron 2 is incident ($\varepsilon_2 < 0$), θ_2 is measured relative to θ_1 (by symmetry only $\theta_2 - \theta_1$ matters), and z_1 specifies the position (or phase) of bound electron 1 when the evolution begins. The functions ε_+ and ρ_+ are the energy and radial position of the electron with the largest energy in the post-collision state. Likewise, one can define the backward transition rate

$$k_-(\rho_1,\varepsilon_1|\bar{\rho},\bar{\varepsilon})$$
$$= n_e b^3 \frac{1}{\tau_1} \oint_{\varepsilon_1} \frac{dz_1}{v_1} \int \rho_2\, d\rho_2\, d\theta_2\, dv_2\, |v_2|\, f_{\rm th}(\varepsilon_2)$$
$$\times \delta[\bar{\varepsilon} - \varepsilon_-(z_1,\rho_1,\varepsilon_1,\rho_2,\theta_2,\varepsilon_2)]$$
$$\times \delta[\bar{\rho} - \rho_-(z_1,\rho_1,\varepsilon_1,\rho_2,\theta_2,\varepsilon_2)], \tag{16b}$$

where the minus indicates evolution backward in time from an initial state characterized by $(z_1,\rho_1,\varepsilon_1,\rho_2,\theta_2,\varepsilon_2)$. The functions ε_- and ρ_- are the energy and radial position of the electron with the largest energy in the pre-collision state; these quantities may be identified with ε' and ρ' in Eq. (15). By time-reversal symmetry (reversal of all velocities), it follows that $k_-(\rho_1,\varepsilon_1|\bar{\rho},\bar{\varepsilon}) = k_+(\rho_1,\varepsilon_1|\bar{\rho},\bar{\varepsilon})$; so we may drop the plus and minus.

In terms of this rate, Eq. (15) takes the form

$$\frac{\partial \bar{f}_1(\rho,\varepsilon)}{\partial t} = \int d\bar{\rho}\, d\bar{\varepsilon}\, f_{\rm th}(\varepsilon)\, k(\rho,\varepsilon,|\bar{\rho},\bar{\varepsilon}) \left(\frac{\bar{f}_1(\bar{\rho},\bar{\varepsilon})}{f_{\rm th}(\bar{\varepsilon})} - \frac{\bar{f}_1(\rho,\varepsilon)}{f_{\rm th}(\varepsilon)} \right), \tag{17a}$$

where we have dropped the subscript on ε_1 and ρ_1. To put this in the standard form for a master equation, it is useful to introduce the distribution $W(\rho,\varepsilon) = n_e b^3 2\pi\rho\tau(\rho,\varepsilon)\, \bar{f}_1$

$\times(\rho,\varepsilon)$, where $n_e b^3 2\pi\rho\tau(\rho,\varepsilon)$ is the density of states for the differential $d\rho\, d\varepsilon$. Equation (17a) then takes the form

$$\frac{\partial W(\rho,\varepsilon)}{\partial t} = \int d\bar{\rho}\, d\bar{\varepsilon}\, W_{\rm th}(\rho,\varepsilon)\, k(\rho,\varepsilon|\bar{\rho},\bar{\varepsilon}) \times\left(\frac{W(\bar{\rho},\bar{\varepsilon})}{W_{\rm th}(\bar{\rho},\bar{\varepsilon})} - \frac{W(\rho,\varepsilon)}{W_{\rm th}(\rho,\varepsilon)}\right), \tag{17b}$$

where $W_{\rm th}(\rho,\varepsilon) = (n_e b^3) 2\pi\rho\tau(\rho,\varepsilon) f_{\rm th}(\varepsilon)$. By using time-reversal symmetry plus the Liouville theorem one obtains the statement of detailed balance[14,16]

$$W_{\rm th}(\rho,\varepsilon) k(\rho,\varepsilon|\bar{\rho},\bar{\varepsilon}) = W_{\rm th}(\bar{\rho},\bar{\varepsilon}) k(\bar{\rho},\bar{\varepsilon}|\rho,\varepsilon). \tag{18}$$

Also, one can verify this relation by noting that it is required for Eq. (17b) to conserve particle number for an arbitrary choice of $W(\rho,\varepsilon)$. Substituting this relation into Eq. (17b) then yields the master equation[16]

$$\frac{\partial W(\rho,\varepsilon)}{\partial t} = \int d\bar{\rho}\, d\bar{\varepsilon}\, [k(\bar{\rho},\bar{\varepsilon}|\rho,\varepsilon) W(\bar{\rho},\bar{\varepsilon}) - k(\rho,\varepsilon|\bar{\rho},\bar{\varepsilon}) W(\rho,\varepsilon)]. \tag{19}$$

III. FOKKER–PLANCK EQUATION

In this section, we focus on collisions characterized by an impact parameter that is somewhat larger than b and reduce Eqs. (6) and (9) to a Fokker–Planck equation. Consider the case where electron 1 is bound ($\varepsilon_1 > 0$) at a radius $\rho_1 < 1$ and electron 2 is incident from infinity ($\varepsilon_2 < 0$) at a relatively large radius $\rho_2 \gtrsim \rho_d \gg 1$. Here, the cutoff at $\rho_2 \cong \rho_d$ is introduced arbitrarily; one might imagine that an opaque disk of radius ρ_d is placed in front of each ion. For this situation, Eq. (6) can be solved perturbatively through an expansion in $1/\rho_2$, that is, through an expansion in the weakness of the interactions ϕ_{12} and ϕ_{20}. To simplify the analysis, we can assume that electron 1 is bound deeply enough that its oscillatory motion is simple harmonic.

It is useful to rewrite Eq. (6) as $(L^{(0)} + L^{(1)}) f_2 = 0$, where

$$L^{(0)} = \frac{\partial}{\partial t} + v_1 \frac{\partial}{\partial z_1}\bigg|_{\varepsilon_1} + v_2 \frac{\partial}{\partial z_2}\bigg|_{v_2}, \tag{20a}$$

$$L^{(1)} = -\frac{\partial\phi_{12}}{\partial z_1} v_1 \frac{\partial}{\partial\varepsilon_1} - \left(\frac{\partial\phi_{12}}{\partial z_2} + \frac{\partial\phi_{20}}{\partial z_2}\right)\frac{\partial}{\partial v_2}, \tag{20b}$$

and v_2, rather than ε_2, is treated as an independent variable. The zeroth-order orbits described by $L^{(0)}$ are such that electron 1 oscillates back and forth with a constant value of ε_1 and electron 2 streams by with a constant value of v_2. At first glance, the operator $L^{(1)}$ appears to be of mixed order in the expansion parameter $1/\rho_2$. The quantity $\partial\phi_{12}/\partial z_1$ is of order $1/\rho_2^2$; whereas, the bracket $(\partial\phi_{12}/\partial z_2 + \partial\phi_{20}/\partial z_2)$ is of order $1/\rho_2^3$, since ϕ_{12} and ϕ_{20} cancel to lowest order leaving a dipole interaction. However, we will find that the two terms in $L^{(1)}$ contribute equally. The reason is that the derivative $\partial/\partial v_2$ will produce a factor v_2 (i.e., $\partial/\partial v_2 = v_2\,\partial/\partial\varepsilon_2$) and this factor is effectively of order ρ_2.

Let us look for a solution of the form $f_2 = f_2^{(0)} + f_2^{(1)}$, where

$$f_2^{(0)}(1,2) = \bar{f}_1(\rho_1,\varepsilon_1)\left(e^{-v_2^2/2}/\sqrt{2\pi}\right). \tag{21}$$

This choice for $f_2^{(0)}$ is determined not only by the requirement that $L^{(0)} f_2^{(0)} = 0$, but also by the requirement that electrons 1 and 2 are uncorrelated in zero order, and by the fact that electron 2 is unbound and hence distributed thermally. The first-order distribution is determined by the equation

$$L^{(0)} f_2^{(1)} = -L^{(1)} f_2^{(0)}, \tag{22}$$

where second-order term $L^{(1)} f_2^{(1)}$ has been neglected. The operator $L^{(0)}$ is the total time derivative taken along the zeroth-order orbits; so a solution for $f_2^{(1)}$ is given by an integral over these orbits

$$f_2^{(1)} = +\int_{-\infty}^{t} dt' \left[\left(\frac{\partial\phi_{12}}{\partial z_1} v_1\right)' \frac{\partial\bar{f}_1}{\partial\varepsilon_1}(\rho_1,\varepsilon_1) \frac{e^{-v_2^2/2}}{\sqrt{2\pi}} - \left(\frac{\partial\phi_{12}}{\partial z_2} + \frac{\partial\phi_{20}}{\partial z_2}\right)' v_2 \frac{e^{-v_2^2/2}}{\sqrt{2\pi}} \bar{f}_1(\rho_1,\varepsilon_1)\right]. \tag{23}$$

The zero-order orbits are given by

$$\varepsilon_1(t') = \varepsilon_1, \quad v_2(t') = v_2, \quad z_2(t') = z_2 + v_2(t'-t), \tag{24}$$

$$z_1(t') = a_1 \cos[\psi_1(t')], \quad \psi_1(t') = \psi_1 + \omega_1(t'-t),$$

where the amplitude of oscillation of particle 1 is given by $\omega_1^2 a_1^2/2 = (1/\rho_1 - \varepsilon_1)$ and the frequency by $\omega_1^2 = 1/\rho_1^3$. This follows from the deep binding approximation for the energy of particle 1, $\varepsilon_1 \cong 1/\rho_1 - [v_1^2/2 + (1/\rho_1^3) z_1^2/2]$.

Substituting Eq. (23) into Eq. (9) yields the Fokker–Planck equation

$$\tau_1 \frac{\partial\bar{f}_1}{\partial t} = -\frac{\partial}{\partial\varepsilon_1}\left(B\bar{f}_1(\rho_1,\varepsilon_1) + A\frac{\partial\bar{f}_1}{\partial\varepsilon_1}(\rho_1,\varepsilon_1)\right), \tag{25}$$

where

$$A = +n_e b^3 \tau_1 \int_0^{2\pi}\frac{d\psi_1}{2\pi}\int d\mathbf{r}_2 \int_{-\infty}^{+\infty} dv_2 \int_{-\infty}^{t} dt' \frac{e^{-v_2^2/2}}{\sqrt{2\pi}} \times\left(v_1\frac{\partial\phi_{12}}{\partial z_1}\right)\left(v_1\frac{\partial\phi_{12}}{\partial z_1}\right)', \tag{26a}$$

$$B = -n_e b^3 \tau_1 \int_0^{2\pi}\frac{d\psi_1}{2\pi}\int d\mathbf{r}_2 \int_{-\infty}^{+\infty} dv_2 \int_{-\infty}^{t} dt' \frac{e^{-v_2^2/2}}{\sqrt{2\pi}} \times v_2\left(v_1\frac{\partial\phi_{12}}{\partial z_1}\right)\left(\frac{\partial\phi_{12}}{\partial z_2} + \frac{\partial\phi_{20}}{\partial z_2}\right)', \tag{26b}$$

and the integral $\oint dz_1/v_1$ has been replaced by $\tau_1\int_0^{2\pi} d\psi_1/2\pi$. To evaluate A, we approximate $\partial\phi_{12}/\partial z_1$ by $z_2/(z_2^2+\rho_2^2)^{3/2}$, use the identity

$$\frac{z}{(z^2+\rho^2)^{3/2}} = \frac{2}{\pi}\int_0^\infty dk\, k\, K_0(k\rho)\sin kz, \tag{27}$$

and substitute the orbits in Eq. (24). The result is the integral expression

$$A = +n_e b^3 \tau_1 \int_0^{2\pi}\frac{d\psi_1}{2\pi}\int_{-\infty}^{+\infty} dz_2 \int_{\rho_d}^{\infty} 2\pi\rho_2\, d\rho_2 \int_{-\infty}^{+\infty} dv_2 \times\int_{-\infty}^{t} dt'\left(\frac{2}{\pi}\right)^2 \int_0^\infty dk\, k \int_0^\infty dq\, q \frac{e^{-v_2^2/2}}{\sqrt{2\pi}} K_0(k\rho_2) \times K_0(q\rho_2)(a_1\omega_1)^2 \sin\psi_1 \sin[\omega_1(t'-t)+\psi_1] \times\sin kz_2 \sin[qz_2 + qv_2(t'-t)]. \tag{28}$$

where a low impact parameter cutoff has been introduced at $\rho_2 = \rho_d$. Carrying out the z_2, ψ_1, q, t', and k integrals in that order then yields the result

$$A = +n_e b^3 \tau_1 (a_1\omega_1)^2 \frac{8\pi}{\sqrt{2\pi}} \int_0^\infty \frac{dv_2}{v_2} \times e^{-v_2^2/2} \int_{(\omega_1\rho_d/v_2)}^\infty d\xi\, \xi\, K_0^2(\xi). \tag{29}$$

In evaluating B, one must pay attention to the fact that ϕ_{12} and ϕ_{20} cancel to lowest order leaving a dipole interaction. Applying identity (27) to $\partial\phi_{12}/\partial z_2 = (z_1 - z_2)/|\mathbf{r}_1 - \mathbf{r}_2|^3$ and to $\partial\phi_{20}/\partial z_2 = z_2/|\mathbf{r}_2|^3$ yields the approximate relation

$$\left(\frac{\partial\phi_{12}}{\partial z_2} + \frac{\partial\phi_{20}}{\partial z_2}\right) \cong \frac{2}{\pi}\int_0^\infty dq\, q\, K_0(q\rho_{12})(qz_1 \cos qz_2 - \sin qz_2) + \frac{2}{\pi}\int_0^\infty dq\, q\, K_0(q\rho_2)\sin kz_2, \tag{30}$$

which is accurate to order $1/\rho_2^3$. Also, using identity (27) to evaluate $\partial\phi_{12}/\partial z_1 \cong z_2/(z_2^2 + \rho_2^2)^{3/2}$, substituting for the zeroth-order orbits, and evaluating the z_2, ψ_1, q, and t' integrals in that order yields the result $B = A$; so Eq. (25) reduces to

$$\tau_1 \frac{\partial\bar{f}_1}{\partial t} = -\frac{\partial}{\partial\varepsilon_1}\left[A\left(\bar{f}_1 + \frac{\partial\bar{f}_1}{\partial\varepsilon_1}\right)\right]. \tag{31}$$

Of course, this result would have been anticipated since the bracket on the right must vanish for a thermal distribution [Eq. (10)].

What conclusions can be drawn from this simple calculation? First, we note that A is exponentially small for sufficiently large ρ_d. By using the large ξ asymptotic expansion $K_0(\xi) = (\pi/2\xi)^{1/2}\exp(-\xi)$ and evaluating the v_2 integral with the saddle point method, Eq. (29) reduces to the form

$$A = +n_e b^3 \tau_1 (a_1\omega_1)^2 \frac{2\pi^2}{\sqrt{3}} \frac{e^{-3/2(2\omega_1\rho_d)^{2/3}}}{(2\omega_1\rho_d)^{1/3}}. \tag{32}$$

In terms of unscaled variables the argument of the exponential is given by $(2\omega_1\rho_d)^{2/3} \to (2\omega_1\rho_d/v_e)^{2/3}$. The exponential cutoff is simply a manifestation of an adiabatic invariant for the oscillatory motion of electron 1. This invariant is nearly conserved when the interaction field is slowly varying (i.e., $\omega_1 \gg v_e/\rho_d$). Note that the existence of this invariant is not associated with the approximation that electron 1 is bound tightly enough that its oscillatory motion is simple harmonic. The result can be generalized by using action angle variables.

Another conclusion follows from the observation that A is sensitive to the value of ρ_d when ρ_d is pushed down to the range $\rho_d \cong 1$ where the expansion procedure fails. This means that small impact parameter collisions make a significant contribution and the Fokker–Planck treatment is not the whole story.

Incidentally, the analysis can be carried out when the $\mathbf{E}\times\mathbf{B}$ drift motion is retained, and a correction to A of order $\delta A \sim (r_{ce}/b)^2 A$ is found. The smallness of the correction is simply a verification of the fact that this motion is negligible.

IV. VARIATIONAL THEORY AND THE KINETIC BOTTLENECK

The variational theory of three-body recombination[15] can be thought of as the opposite limit from the Fokker–Planck theory; the distribution function is assumed to vary sharply compared to a step size. Anticipating the existence of a bottleneck, the variational theory presumes that the distribution $f_2(1,2)$ is zero for $\varepsilon_1 > \varepsilon$ and is of the thermal equilibrium form

$$f_2(1,2) = (1/2\pi)e^{\varepsilon_1 + \varepsilon_2 - \phi_{12}} \tag{33}$$

for $\varepsilon_1 < \varepsilon$. Here, electron 1 is bound and electron 2 is a free electron that interacts with electron 1; the value of ε is ultimately chosen to be the energy location of the bottleneck. The theory requires a specification of $f_2(1,2)$ on the surface $\varepsilon_1 = \varepsilon$, and from Eq. (6) one can see the term $v_1(\partial\phi_{12}/\partial z_1)(\partial f_2/\partial\varepsilon_1)$ convects the thermal form of f_2 to the surface for $v_1\,\partial\phi_{12}/\partial z_1 > 0$ and convects the zero value to the surface for $v_1\,\partial\phi_{12}/\partial z_1 < 0$.

The first step is to calculate the flux of electrons through the surface $\varepsilon_1 = \varepsilon$. From Eq. (9) and from the relation

$$\frac{dN}{d\varepsilon_1} = n_e b^3 \int d\mathbf{r}_{1\perp} \oint_{\varepsilon_1} \frac{dz_1}{v_1} \bar{f}_1(\rho_1,\varepsilon_1) \tag{34}$$

one can see that the dimensionless flux toward deeper binding through the surface $\varepsilon_1 = \varepsilon$ is given by

$$R(\varepsilon) = (n_e b^3)^2 \int d\mathbf{r}_{1\perp} \oint_{\varepsilon_1=\varepsilon} \frac{dz_1}{v_1} \times \int d\mathbf{r}_2\, dv_2\, v_1 \frac{\partial\phi_{12}}{\partial z_1} f_2(1,2). \tag{35}$$

Here, the distribution $f_2(1,2)$ is taken to be of the thermal equilibrium form for $v_1\,\partial\phi_{12}/\partial z_1 > 0$ and to be zero for $v_1\,\partial\phi_{12}/\partial z_1 < 0$. In the (z_1, v_1) phase space, the loop defined by $\varepsilon_1 = \varepsilon$ is such that $v_1 > 0$ for the top half and $v_1 < 0$ for the bottom half. Consequently, $v_1\,\partial\phi_{12}/\partial z_1 > 0$ at any point z_1 for either the top or the bottom of the loop, and Eq. (35) can be rewritten as

$$R(\varepsilon) = (n_e b^3)^2 \int d\mathbf{r}_{1\perp} \int dz_1 \int d\mathbf{r}_2\, dv_2 \left|\frac{\partial\phi_{12}}{\partial z_1}\right| f_2, \tag{36}$$

where f_2 is of the thermal equilibrium form and is evaluated for $\varepsilon_1 = \varepsilon$. The integral over z_1 is over one half the loop in the direction of increasing z_1 (i.e., $-\sqrt{\varepsilon^{-2} - r_{1\perp}^2} < z_1 < \sqrt{\varepsilon^{-2} - r_{1\perp}^2}$).

Also, we restrict the domain of integration to the regime where $\varepsilon_1 + \varepsilon_2 - \phi_{12} < \varepsilon_1$; this insures that it is energetically possible for electron 1 to move from $\varepsilon_1 = \varepsilon$ to deeper binding and for electron 2 to escape to infinity. This restriction can be rewritten as a restriction on the domain of the v_2 integration (i.e., $v_2^2/2 + \phi_{12} + \phi_{20} > 0$).

One final restriction is necessary. Large impact parameter collisions produce small steps in the binding energy, some positive and some negative, and as we have seen, the evolution due to these collisions is diffusive in nature. In addition, large impact parameter collisions tend to have recrossings of the surface $\varepsilon_1 = \varepsilon$ during the course of a collision. The one-way thermal equilibrium flux being calculated here would greatly overestimate the contribution from these

collisions; in fact, the contribution would diverge. For that reason, the integral in Eq. (36) is cut off for $|\mathbf{r}_2 - \mathbf{r}_1| \gtrsim C/\varepsilon$, where C is a constant. To understand the scaling with ε, note that $|\mathbf{r}_1|_{\max} = 1/\varepsilon$ and that $|\mathbf{r}_2 - \mathbf{r}_1|$ must be less than on the order of $|\mathbf{r}_1|_{\max}$ for the interaction to make a substantial change in the atomic state.

It is convenient to change variables from $(\mathbf{r}_1,\mathbf{r}_2)$ to $(\bar{r}_1,\zeta,\psi,\bar{r}_{21},\theta,\phi)$ where

$$(\mathbf{r}_2 - \mathbf{r}_1) = \bar{r}_{21}\varepsilon^{-1}(\sin\theta\cos\phi\,\hat{x} + \sin\theta\sin\phi\,\hat{y} + \cos\theta\,\hat{z}), \tag{37}$$

$$\mathbf{r}_1 = \bar{r}_1\varepsilon^{-1}(\sin\zeta\cos\psi\,\hat{x}' + \sin\zeta\sin\psi\,\hat{y}' + \cos\zeta\,\hat{z}'),$$

and

$$\begin{aligned}\hat{z}' &= \sin\theta\cos\phi\,\hat{x} + \sin\theta\sin\phi\,\hat{y} + \cos\theta\,\hat{z},\\ \hat{y}' &= -\sin\phi\,\hat{x} + \cos\phi\,\hat{y},\\ \hat{x}' &= \cos\theta\cos\phi\,\hat{x} + \cos\theta\sin\phi\,\hat{y} - \sin\theta\,\hat{z}.\end{aligned} \tag{38}$$

An important point to note is that $\hat{z}'$ is directed along the $(\mathbf{r}_2 - \mathbf{r}_1)$ direction; so ζ is the angle between $(\mathbf{r}_2 - \mathbf{r}_1)$ and $\mathbf{r}_1$. Rewriting Eq. (36) in terms of these variables, taking into account the restrictions on the domain of integration, and carrying out the v_2 integration yields the result

$$\begin{aligned}R(\varepsilon) = (n_e b^3)^2 \frac{e^{\epsilon}}{2\pi\varepsilon^4}&\int_0^C d\bar{r}_{21}\,\bar{r}_{21}^2\int_0^{\pi}\sin\theta\,d\theta\int_0^{2\pi}d\phi\\ &\times\int_0^1 d\bar{r}_1\,\bar{r}_1^2\int_0^{\pi}\sin\zeta\,d\zeta\int_0^{2\pi}d\psi\,\frac{|\cos\theta|}{\bar{r}_{21}^2}\\ &\times e^{\mu}\sqrt{2\pi}\,F(\mu),\end{aligned} \tag{39}$$

where $F(\mu) = \operatorname{erfc}(\sqrt{\max(\mu,0)})$ and

$$\mu = \varepsilon\left(\frac{1}{\sqrt{\bar{r}_1^2 + \bar{r}_{21}^2 - 2\bar{r}_1\bar{r}_{21}\cos\zeta}} - \frac{1}{\bar{r}_{21}}\right). \tag{40}$$

The integrations over all angles except ζ can be carried out trivially and yield

$$R(\varepsilon) = (n_e b^3)^2\frac{e^{\epsilon}}{\varepsilon^4}(2\pi)^{3/2}\int_0^C d\bar{r}_{21}\int_0^1 d\bar{r}_1\,\bar{r}_1^2\int_{-1}^1 dx\,e^{\mu}F(\mu), \tag{41}$$

where $x = \cos\zeta$.

The behavior of $R(\varepsilon)$ can be examined by looking at an upper bound. Using the inequality $F(\mu)e^{\mu} \leqslant 1$ in Eq. (41) and carrying out the integrals yields

$$R(\varepsilon) \leqslant (n_e b^3)^2 C\frac{e^{\epsilon}}{\varepsilon^4}\frac{2(2\pi)^{3/2}}{3}. \tag{42}$$

The minimum value of the right-hand side is approximately $(2.2)C(n_e b^3)^2$ and is attained at $\varepsilon = 4$. This strong minimum in the one-way thermal equilibrium flux is called the bottleneck; it is due to a competition between the Boltzmann factor e^{ϵ} and the phase space factor ε^{-4}. The variational theory takes the value of the flux at the bottleneck to be the recombination rate.

A more accurate evaluation of Eq. (41) can be carried out numerically. Such evaluations have been used to minimize $R(\varepsilon)$ for various values of C, and the results are shown in Figs. 2 and 3. Figure 2 shows the location of the minimum (or bottleneck) ε_b. As one would expect from Eq. (42), the location of the minimum in $R(\varepsilon)$ is insensitive to the value of C and has the approximate value $\varepsilon_b \cong 4$. Figure 3 displays the value of the minimum flux. The bound on the minimum flux Eq. (42) is always greater than the calculated value, as we would expect. In addition, the minimum flux scales as C to the first power as C goes to infinity—the same as the upper bound.

The variational theory illustrates the idea of a bottleneck and provides an order of magnitude estimate of the recombination rate but does not provide an accurate value of the rate. First, the theory has a free parameter, C, to compensate for recrossings. Although the Fokker–Planck analysis suggests that C is of order unity, its precise value is not known. Second, the bottleneck is not infinitely sharp but extends over some finite range $\Delta\varepsilon \sim O(1)$. At the low ε end of this range, the atomic states are populated according to

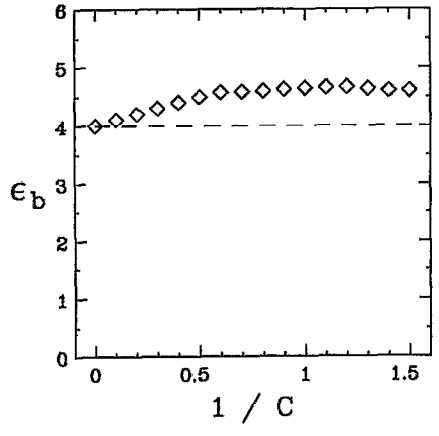

FIG. 2. Energy that gives the minimum flux (i.e., the location of the bottleneck) as a function of the adiabatic cutoff used in the integration. The dashed line shows the estimate of $\varepsilon_b = 4$ predicted by Eq. (42). The quantity C is the adiabatic cutoff defined in Sec. IV

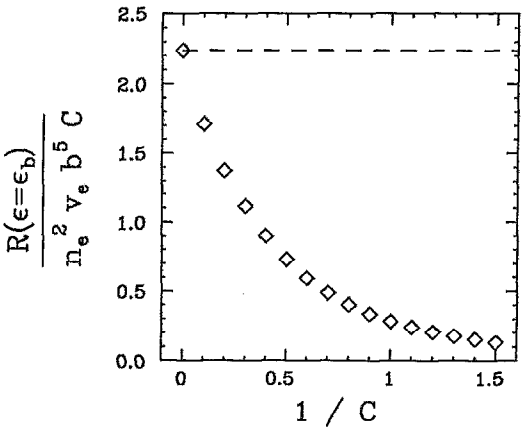

FIG. 3. The minimum value of the one-way thermal equilibrium flux as a function of adiabatic cutoff used. The dashed line is the upper bound given by Eq. (42). Note that for large values of the adiabatic cutoff C, the one-way thermal equilibrium flux approaches the upper bound.

thermal equilibrium, but the flux is not predominantly one way. At the high ε end, the flux is predominantly toward deeper binding but the atomic states are depleted relative to thermal equilibrium. There is no one surface where the states are populated according to thermal equilibrium and the flux is predominantly one way. Finally, the theory assumes that the surface defining the bottleneck depends only on ε, rather than on ε and ρ. Such an assumption makes sense when the transitions between ρ values are more rapid than those between ε values, but this is not the case where a strong magnetic field is present.

V. MONTE CARLO SIMULATION

This section presents a numerical simulation of the recombination process and a numerical determination of the rate. The simulation traces the state of an atom through a sequence of collisions with electrons from the background plasma. The distribution of atomic states is assumed to be of the thermal equilibrium form down to some energy $\varepsilon_{\rm th} > 0$. We will choose $\varepsilon_{\rm th}$ to be substantially smaller than the bottleneck energy $\varepsilon_b \sim 4$ and will find from the numerical results themselves that the thermal distribution extends below $\varepsilon_{\rm th}$. To initiate the simulation, an electron in an initial state chosen at random from the thermal distribution for the background plasma is allowed to collide with an atom in an initial state chosen at random from the thermal distribution of atomic states (i.e., $\varepsilon < \varepsilon_{\rm th}$). This process is repeated until an atom is formed with binding energy greater than $\varepsilon_{\rm th}$. The state of this atom is then followed through a sequence of collisions with electrons chosen at random from the thermal distribution for the background plasma. The simulation stops following the atomic state, when the state goes back into the thermal distribution ($\varepsilon < \varepsilon_{\rm th}$) or reaches the sink ($\varepsilon > \varepsilon_s$). We will choose ε_s to be substantially larger than the bottleneck energy ($\varepsilon_s \gg \varepsilon_b$) and will find from the numerical results themselves that it is very unlikely for an atom to be reionized once it has passed beyond the bottleneck. An atom that reaches the sink is declared to be recombined, and the steady-state flux to the sink is the recombination rate.

Formally one may think of this simulation as a Monte Carlo solution of the master equation, Eq. (19). This equation describes a Markov process[16] with transition rates $k(\rho,\varepsilon|\bar{\rho},\bar{\varepsilon})$. The evolution of a guiding center atom in the state (ρ,ε) is governed by the probability that the earliest change in state is at a time between t and $t+dt$ to a state with energy between $\bar{\varepsilon}$ and $\bar{\varepsilon}+d\bar{\varepsilon}$ and radial position between $\bar{\rho}$ and $\bar{\rho}+d\bar{\rho}$

$$P(\bar{\rho},\bar{\varepsilon},t)\,d\bar{\varepsilon}\,d\bar{\rho}\,dt = k(\rho,\varepsilon|\bar{\rho},\bar{\varepsilon})\,e^{-R(\rho,\varepsilon)t}\,d\bar{\rho}\,d\bar{\varepsilon}\,dt, \quad (43)$$

where the total collision rate $R(\rho,\varepsilon)$ is given by

$$R(\rho,\varepsilon) = \int k(\rho,\varepsilon|\bar{\rho},\bar{\varepsilon})\,d\bar{\rho}\,d\bar{\varepsilon}. \quad (44)$$

Such an evolution, where the next step is dependent only on the current state rather than the past history, is what we mean by a Markov process. The Monte Carlo aspect of the simulation is the determination of the time of the transition and of the final state by a random choice weighted according to $P(\bar{\rho},\bar{\varepsilon},t)$.

The choice of $(\bar{\rho},\bar{\varepsilon})$ and t is complicated by the expression for the transition rate, Eq. (16a), which is not a simple function of $\bar{\rho}$ and $\bar{\varepsilon}$. It is dependent on the functions $\rho_+(z,\rho,\varepsilon,\rho_2,\theta_2,\varepsilon_2)$ and $\varepsilon_+(z,\rho,\varepsilon,\rho_2,\theta_2,\varepsilon_2)$ that must be determined by numerical integration of the equations of motion. (Here, we have replaced z_1,ρ_1,ε_1 by z,ρ,ε.) Although it is convenient to have a simple expression for the transition rate, it suffices to have a numerical method of choosing $(\bar{\rho},\bar{\varepsilon})$ in a manner consistent with the distribution $k(\rho,\varepsilon|\bar{\rho},\bar{\varepsilon})$. To this end, we choose the pre-collision variables in a manner dictated by the weighing factor in the transition rate, that is,

$$P(z,\rho_2,\theta_2,v_2)\,dz\,d\rho_2\,d\theta_2\,dv_2 = \frac{\rho_2\,d\rho_2\,d\theta_2\,|v_2|\,f_{\rm th}(\varepsilon_2)\,dv_2\,dz/v(z,\rho,\varepsilon)}{\int\rho_2\,d\rho_2\,d\theta_2\,dv_2\,|v_2|\,f_{\rm th}(\varepsilon_2)\oint_\varepsilon dz/v(z,\rho,\varepsilon)}. \quad (45)$$

With the initial conditions chosen in this manner, the equations of motion are integrated numerically to determine $(\bar{\rho},\bar{\varepsilon})$, and it is an easy exercise to show that $(\bar{\rho},\bar{\varepsilon})$ so chosen are distributed according to $k(\rho,\varepsilon|\bar{\rho},\bar{\varepsilon})$.

A technical complication arises from the fact that the integral over ρ_2 diverges in the normalization factor above and in the total collision rate

$$R(\rho,\varepsilon) = n_e b^3 \frac{1}{\tau(\rho,\varepsilon)}\oint\frac{dz}{v(z,\rho,\varepsilon)}\int d\rho_2\,\rho_2 \times d\theta_2\,dv_2\,|v_2|\,f_{\rm th}(\varepsilon_2), \quad (46)$$

which is obtained by substituting Eq. (16) into Eq. (44) and carrying out the integrals over the delta functions. However, we know from the Fokker–Planck analysis [see Eq. (32)] that the large ρ_2 collisions contribute an exponentially small amount to the diffusion coefficient. The divergence can be removed without affecting the transport by introducing a cutoff for ρ_2. We take the cutoff to be the larger of the adiabatic cutoff (i.e., the radius at which the product of the z-bounce frequency $\omega_z \sim \varepsilon^{-3/2}$ and the collision time $t_c \sim \rho/v_2$ is much greater than one) and the maximum radius at which an electron can be bound with energy ε (i.e., $\rho = \varepsilon^{-1}$). The second condition is necessary so that we can make the dipole approximation for the interaction potential ϕ_{12} as was done in the Fokker–Planck analysis. The cutoff can be stated simply as

$$\rho_c(\varepsilon,v_2) = C'\max(\varepsilon^{-3/2}v_2,\varepsilon^{-1}), \quad (47)$$

where C' is some constant. We choose C' to be large enough that the results of the Monte Carlo simulation are insensitive to further increase in C'.

We now wish to obtain a set of possible realizations for the temporal evolution of the state of a bound atom. To get one possible evolution we need to follow an atom through a sequence of collisions with electrons. The choice of initial state for the atom requires some explanation. Since unbound electrons stream in from infinity, where the plasma is specified to be in thermal equilibrium, we know that the distribution of states is of the thermal equilibrium form for $\varepsilon < 0$. Also, there is rapid thermalization of the weakly bound states ($\varepsilon \gtrsim 0$) and, in steady state, thermalization down to near the bottleneck energy $\varepsilon_b \sim 4$. For the numerical work, we assume that the distribution of atomic states is thermal down to some small but positive binding energy

$\varepsilon_{\rm th}$ $(0<\varepsilon_{\rm th}<\varepsilon_b)$. We choose $\varepsilon_{\rm th}$ to be large enough that any initial state with $\varepsilon>\varepsilon_{\rm th}$ has a reasonable probability (e.g., 1/400 for $\varepsilon_{\rm th}\approx 1$) of evolving through subsequent collisions to the sink. We consider transitions out of this thermal sea to deeper binding (from $\varepsilon<\varepsilon_{\rm th}$ to $\bar{\varepsilon}>\varepsilon_{\rm th}$). The rate of such transitions into a state $(\bar{\rho},\bar{\varepsilon})$, where $\bar{\varepsilon}>\varepsilon_{\rm th}$, is given by

$$k_{\rm i}(\bar{\rho},\bar{\varepsilon})=\int_{\varepsilon<\varepsilon_{\rm th}} d\rho\, d\varepsilon\, k(\rho,\varepsilon|\bar{\rho},\bar{\varepsilon})\, W_{\rm th}(\rho,\varepsilon), \tag{48}$$

and the total rate for transitions to any state with $\bar{\varepsilon}>\varepsilon_{\rm th}$ is given by

$$R_{\rm i}=\int_{\bar{\varepsilon}>\varepsilon_{\rm th}} d\bar{\rho}\, d\bar{\varepsilon}\, k_{\rm i}(\bar{\rho},\bar{\varepsilon}). \tag{49}$$

Thus, the probability that the earliest transition occurs between t^* and t^*+dt^* and is to a state with energy between $\bar{\varepsilon}_0$ and $\bar{\varepsilon}_0+d\bar{\varepsilon}_0$ and radial position between $\bar{\rho}_0$ and $\bar{\rho}_0+d\bar{\rho}_0$ is given by

$$P(\bar{\rho}_0,\bar{\varepsilon}_0,t^*)\,d\bar{\rho}_0\, d\bar{\varepsilon}_0\, dt^* = k_{\rm i}(\bar{\rho}_0,\bar{\varepsilon}_0)e^{-R_{\rm i}t^*}\, d\bar{\rho}_0\, d\bar{\varepsilon}_0\, dt^*, \tag{50}$$

where the subscript 0 refers to the fact that $(\bar{\rho}_0,\bar{\varepsilon}_0)$ is the initial state in the evolution.

Rather than work with $k_{\rm i}(\bar{\rho},\bar{\varepsilon})$ and $R_{\rm i}$, it is useful (for numerical reasons) to introduce the inverse problem and rely on detailed balance. We will explain the reason for this after the method has been presented. If the states with $\bar{\varepsilon}>\varepsilon_{\rm th}$ were distributed thermally, then the rate of transitions into some state (ρ,ε), where $\varepsilon<\varepsilon_{\rm th}$, would be given by

$$k_{\rm f}(\rho,\varepsilon)=\int_{\bar{\varepsilon}>\varepsilon_{\rm th}} d\bar{\rho}\, d\bar{\varepsilon}\, k(\bar{\rho},\bar{\varepsilon}|\rho,\varepsilon)\, W_{\rm th}(\bar{\rho},\bar{\varepsilon}). \tag{51}$$

Likewise, the total rate into all such states would be given by

$$R_{\rm f}=\int_{\varepsilon<\varepsilon_{\rm th}} d\rho\, d\varepsilon\, k_{\rm f}(\rho,\varepsilon)=\int_{\bar{\varepsilon}>\varepsilon_{\rm th}} d\bar{\rho}\, d\bar{\varepsilon}\, k_{\rm f}^{-1}(\bar{\rho},\bar{\varepsilon}), \tag{52}$$

where

$$k_{\rm f}^{-1}(\bar{\rho},\bar{\varepsilon})\equiv\int_{\varepsilon<\varepsilon_{\rm th}} d\rho\, d\varepsilon\, k(\bar{\rho},\bar{\varepsilon}|\rho,\varepsilon)\, W_{\rm th}(\bar{\rho},\bar{\varepsilon}). \tag{53}$$

From detailed balance [Eq. (18)], it follows that $k_{\rm i}(\bar{\rho},\bar{\varepsilon})=k_{\rm f}^{-1}(\bar{\rho},\bar{\varepsilon})$ and that $R_{\rm f}=R_{\rm i}$. Consequently, the distribution of initial states and times can be rewritten as $P(\bar{\rho}_0,\bar{\varepsilon}_0,t^*)=k_{\rm f}^{-1}(\bar{\rho}_0,\bar{\varepsilon}_0)\exp(-R_{\rm f}t^*)$.

We use a numerical procedure to pick $(\bar{\rho}_0,\bar{\varepsilon}_0)$ according to this distribution. First, define the quantity

$$\Phi=\int_{\rm all\ \varepsilon} d\rho\, d\varepsilon\, k_{\rm f}(\rho,\varepsilon) = (n_e b^3)^2\int_{\bar{\varepsilon}_0>\varepsilon_{\rm th}} 2\pi\bar{\rho}_0\, d\bar{\rho}_0\, d\,\bar{\varepsilon}_0\,\frac{d\bar{z}_0}{v(\bar{z}_0,\bar{\rho}_0,\bar{\varepsilon}_0)} \times f_{\rm th}(\bar{\varepsilon}_0)\int\rho_2\, d\rho_2\, d\theta_2\, dv_2\,|v_2|\, f_{\rm th}(\varepsilon_2), \tag{54}$$

which is the sum (or integral) of the collision frequencies for all of the atoms with $\bar{\varepsilon}_0>\varepsilon_{\rm th}$ (the distribution of states being assumed thermal). The procedure is to choose $(\bar{z}_0,\bar{\rho}_0,\bar{\varepsilon}_0,\rho_2,\theta_2,\varepsilon_2)$ according to their contribution to Φ and then to integrate numerically through the collision to the final $\varepsilon=\varepsilon_+$ $\times(\bar{z}_0,\bar{\rho}_0,\bar{\varepsilon}_0,\rho_2,\theta_2,\varepsilon_2)$ and $\rho=\rho_+(\bar{z}_0,\bar{\rho}_0,\bar{\varepsilon}_0,\rho_2,\theta_2,\varepsilon_2)$. Reject this try if $\varepsilon>\varepsilon_{\rm th}$, but retain it if $\varepsilon<\varepsilon_{\rm th}$. One can show that $(\bar{\rho}_0,\bar{\varepsilon}_0)$ so determined are distributed according to $k_{\rm f}^{-1}\times(\bar{\rho}_0,\bar{\varepsilon}_0)$. Also if N_T is the total number of trys and $N_{\rm f}$ is the number retained, then as N_T becomes large $R_{\rm f}\cong(N_{\rm f}/N_T)\Phi$.

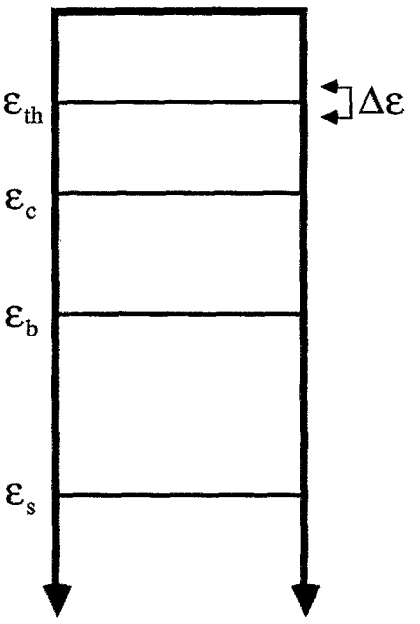

FIG. 4. Relative location of the energies $\varepsilon_{\rm th}$, ε_c, ε_b, and ε_s; and a typical step size $\Delta\varepsilon$.

Technical complications arise again from the fact that the integrals over ρ_2 and $\bar{\varepsilon}_0$ diverge in the expression for Φ [Eq. (54)]. The divergence in ρ_2 can be removed by introducing a cutoff for ρ_2 as we did in Eq. (47). The divergence in $\bar{\varepsilon}_0$ we remove by introducing a lower bound ε_c such that $\varepsilon_c>\varepsilon_{\rm th}$ (see Fig. 4). This cutoff is chosen large enough so that the average change in ε during a collision (i.e., $\langle\Delta\varepsilon\rangle$) is much less than $\varepsilon_c-\varepsilon_{\rm th}$. We check that the results are insensitive to a further increase in ε_c.

One may now ask why did we have to consider the inverse problem when an analogous algorithm could have been defined for the original problem. The answer is efficiency. Most $(\bar{\rho}_0,\bar{\varepsilon}_0)$ chosen in the inverse algorithm are close to $\varepsilon_{\rm th}$, that is, within $\langle\Delta\varepsilon\rangle$. In addition, the transitions normally lead to a smaller value for ε compared to $\bar{\varepsilon}_0$. This implies that most transitions have $\varepsilon<\varepsilon_{\rm th}$, leading to few rejections. The opposite would be true of a forward algorithm. Most initial (ε,ρ) would not be within $\langle\Delta\varepsilon\rangle$ of $\varepsilon_{\rm th}$ and transitions would normally lead to a smaller value for $\bar{\varepsilon}_0$ when compared to ε. Hence most transitions would have $\bar{\varepsilon}_0<\varepsilon_{\rm th}$, leading to many rejections. It is therefore preferable to use the inverse algorithm.

Once we have the initial state $(\bar{\rho}_0,\bar{\varepsilon}_0)$ we continue to follow the evolution through a sequence of collisions until the bound electron is re-ionized or enters the sink. The procedure is then repeated many times with the initial time (t^*) of each evolution measured relative to the initial time of the previous evolution. This ensures that the flux through $\varepsilon=\varepsilon_{\rm th}$ is given by $R_{\rm i}$. We refer to a sequence of $N_{\rm f}$ such

evolutions as a time history for one member of the ensemble of plasmas. Figure 5 shows a graphical representation of a sample time history.

There are three well-separated time scales in a time history. The smallest of these is the duration of a collision: $(v_e/b)^{-1}$ in unscaled variables and unity in scaled variables. (Figure 5 is drawn as though a collision were instantaneous.) The second is the time between collisions: $(n_e b^2 v_e)^{-1}$ in unscaled variables and $(n_e b^3)^{-1}$ in scaled variables. This is the time scale for the duration of an evolution. The third is the time for an electron to make a transition out of the thermal sea to a state with $\varepsilon > \varepsilon_{\rm th}$: $(n_e^2 b^5 v_e)^{-1}$ in unscaled variables and $(n_e b^3)^{-2}$ in scaled variables. This is the time between evolutions. Since the plasma is weakly correlated (i.e., $n_e b^3 \ll 1$), the three time scales are ordered as $(v_e/b)^{-1} \ll (n_e v_e b^2)^{-1} \ll (n_e^2 b^5 v_e)^{-1}$. In other words, a collision is complete before another begins and an evolution is complete before another begins.

Each member of the ensemble of plasmas has an associated time history, and the distribution function $W(\rho,\varepsilon,t)$ that appears in the master equation [i.e., Eq. (19)] can be constructed as an ensemble average over the time histories.

The boundary conditions on the integrodifferential master equation are $W(\rho,\varepsilon,t) = W_{\rm th}(\rho,\varepsilon)$ for $\varepsilon < \varepsilon_{\rm th}$ and $W(\rho,\varepsilon,t) = 0$ for $\varepsilon > \varepsilon_s$. These are enforced by the method by which initial states $(\bar{\rho}_0,\bar{\varepsilon}_0)$ are chosen and the removal of atoms which reach the sink. The initial condition on $W(\rho,\varepsilon,t)$ between $\varepsilon_{\rm th}$ and ε_s is $W(\rho,\varepsilon,t=0) = 0$. This initial condition is built into the time history since no evolution can start before $t = 0$.

By invoking the equality of the temporal average and the ensemble average, we can obtain steady-state quantities from a single time history. For example, the steady-state flux to the sink (the recombination rate) is given by $R_3 = R_s = \Phi N_s/N_T$, where N_s is the number of the initial tries which reach the sink in the course of their subsequent evolution. Likewise, the steady-state distribution is given by

$$W_{\rm ss}(\rho,\varepsilon) \approx \frac{R_t}{N_t} \frac{1}{\Delta\varepsilon\,\Delta\rho} \sum_{ij} t_{ij} \Delta\theta(\varepsilon_{ij};\varepsilon,\Delta\varepsilon) \times \Delta\theta(\rho_{ij};\rho,\Delta\rho), \tag{55}$$

where N_t/R_t is the total elapsed time in the time history,

$$\Delta\theta(x;x_0,\Delta x) = \begin{cases} 1, & \text{if } x_0 \leqslant x \leqslant x_0 + \Delta x, \\ 0, & \text{otherwise,} \end{cases}$$

and t_{ij} is the time spent in the jth state in the ith evolution.

Not only can steady state flow rates and distribution functions be obtained; one can estimate the time-dependent distribution function $W(\rho,\varepsilon,t)$. This needs to be examined in order to see how the steady state is established. The straightforward way to do this is to generate many time histories, that is, many realizations of the ensemble of plasmas. One would then count how many of these histories are in a state (ρ,ε) at time t as an estimate of the distribution function. The problem is that very few realizations would be in any given state at any given time; more specifically only $n_e b^3$ of the histories generated. To compound the problem, each time history is very expensive to generate since one must numerically integrate through many collisions. What we

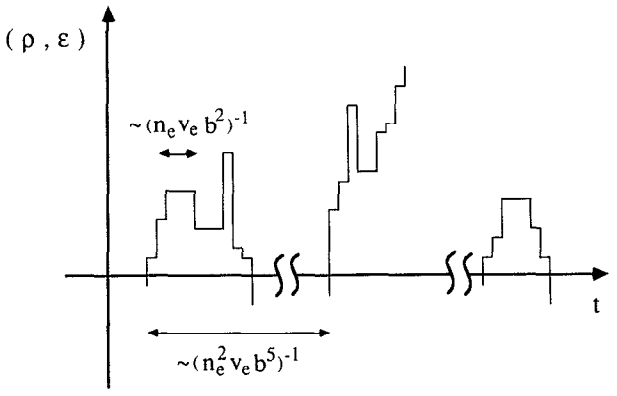

FIG. 5. An example of a time history showing the order of the time scales. The state of the atom (ρ,ε) is plotted as a function of time. The square corners show the duration collision [i.e., $t \sim (v_e/b)^{-1}$] as being effectively instantaneous on the time scale of an evolution. Three evolutions are shown. The duration of an evolution is of order $(n_e v_e b^2)^{-1}$, and the time between evolutions is of order $(n_e^2 v_e b^5)^{-1}$.

choose to do instead is to use one time history and manipulate it to generate a large subensemble of the ensemble of plasmas. An easy way to see how this is done is to first understand that each evolution in a time history is independent of the other evolutions. The time at which an evolution starts is not dependent on the details of that evolution or any other. This will allow us to place the N_t evolutions in the time history at any time between 0 and N_t/R_t with equal probability and to thereby generate an infinite number of realizations of the ensemble. These realizations are a large subensemble that gives us a good estimate of $W(\rho,\varepsilon,t)$. When the average over this subensemble is done one finds that

$$W(\rho,\varepsilon,t) \approx \frac{1}{\Delta\varepsilon\,\Delta\rho} \frac{R_t}{N_t} \sum_{ij} t_{ij}\, \Delta\theta(\varepsilon_{ij};\varepsilon,\Delta\varepsilon) \times \Delta\theta(\rho_{ij};\rho,\Delta\rho)\theta\left(\sum_{l=1}^{j} t_{il}\,;\, t\right), \tag{56}$$

where

$$\theta(x;x_0) = \begin{cases} 1, & \text{if } x \leqslant x_0, \\ 0, & \text{otherwise.} \end{cases}$$

The earlier statement that a temporal average is equal to an ensemble average in steady state can now be justified. Consider a time such that $(n_e b^3)^{-1} \ll t_\infty$. For such a time $\theta(\Sigma_{l=1}^{j} t_{il}; t_\infty) = 1$ for all i and j, so that Eq. (56) reduces to Eq. (55) [i.e., $W(\rho,\varepsilon,t_\infty) = W_{\rm ss}(\rho,\varepsilon)$].

Since we now have an estimate of the time-dependent distribution function, all physically meaningful average quantities can be estimated along with their time dependence. We now present the results of a Monte Carlo simulation. The recombination process is simulated by generating 20 000 evolutions. The value of $\varepsilon_{\rm th}$ used is 1, and the value of ε_c used is 4. The ρ_2 cutoff C' is 4. The following results are found to be insensitive to a further increase in ε_c or C'. The value for which an atom is considered recombined ε_s is 20, well below the expected bottleneck at $\varepsilon_b \sim 4$. Only 1/400 of the evolutions reach ε_s. This corresponds to a numerically calculated recombination rate $R_3 \approx 0.070(10) n_e^2 b^5 v_e$.

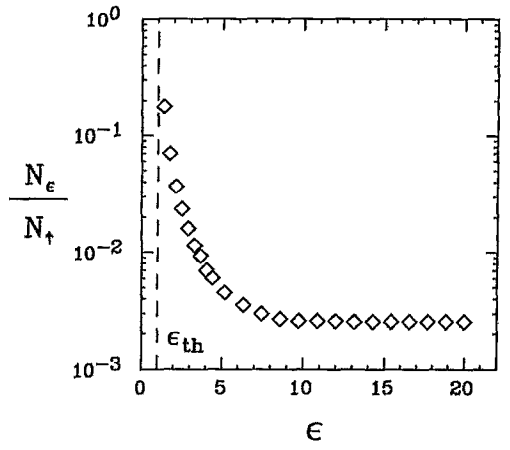

FIG. 6. Number of evolutions which reach ε (i.e., N_ε), divided by the total number of evolutions $N_\uparrow$. This figure shows that one can unambiguously define a recombined atom as an atom which reaches the sink and that a bottleneck of finite width exists near $\varepsilon \sim 4$.

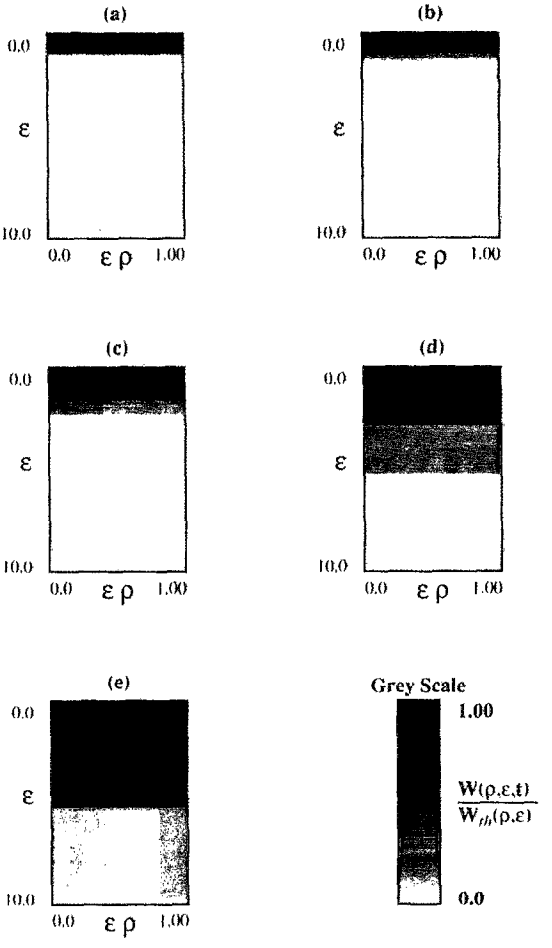

FIG. 7. Time dependent distribution function divided by its thermal value. Shown are its value at four different times (a) $t = 0$ (initial condition), (b) $t = (1/10)(n_e v_e b^2)^{-1}$, (c) $t = (n_e v_e b^2)^{-1}$, (d) $t = 10(n_e v_e b^2)^{-1}$ and its steady-state value (e). All scales are linear.

The existence of the bottleneck is illustrated in Fig. 6. This is a plot (as a function of ε) of the fraction of the evolutions $N_\varepsilon/N_\uparrow$ that make it to the energy ε. Note that almost all, 399 out of 400, of the evolutions lead to re-ionization, but all of the evolutions that make it past $\varepsilon = 10$ eventually reach the sink at ε_s. This allows the unambiguous definition of a recombined atom as one which reaches the sink. It also confirms that there is some energy ε_b between $\varepsilon_{\rm th} = 1$ and $\varepsilon = 10$ such that if an atom is bound with less energy ($\varepsilon < \varepsilon_b$) it is more likely to be ionized and if it is bound with more energy ($\varepsilon > \varepsilon_b$) it is more likely to be recombined. The bottleneck energy ε_b can be determined from Fig. 6 by finding the energy for which the fraction $N_\varepsilon/N_\uparrow$ is twice its constant value for deep binding. This value is found to be $\varepsilon_b \simeq 4.9(10)$, which agrees with the expected bottleneck of $\varepsilon_b = 4$–4.5 shown in Fig. 2. In addition, the finite width of the bottleneck is evidenced by the smooth approach of $N_\varepsilon/N_\uparrow$ to its constant value at deep binding. If the bottleneck was infinitely sharp we would see a discontinuous jump of $N_\varepsilon/N_\uparrow$ at ε_b to its value at deep binding.

The time-dependent distribution function, divided by its thermal equilibrium value $W(\rho,\varepsilon,t)/W_{\rm th}(\rho,\varepsilon)$ is shown in Fig. 7. For convenience we plot this function in $(\varepsilon\rho,\varepsilon)$ space rather than (ρ,ε) space. The maximum value of $\varepsilon\rho$ is unity, so the boundary of the space is rectangular. We display the distribution function for four different times ($tn_e v_e b^2 = 0, 0.1, 1$, and 10) as well as the time asymptotic result ($t = \infty$). The value of the distribution function is indicated by the shade of gray displayed on the $(\varepsilon\rho,\varepsilon)$ plane. Black corresponds to thermal equilibrium and white to total depletion. We first concentrate on the steady state function Fig. 7(e) which remains at its thermal equilibrium value until $\varepsilon = 4$ then precipitously drops off from that value. This again confirms the existence of the bottleneck and justifies the initial formation process with $\varepsilon_{\rm th} = 1$. To more dramatically show the bottleneck, the ρ-integrated time-dependent distribution function

$$W(\varepsilon,t) \equiv \int_0^{1/\varepsilon} d\rho\, W(\rho,\varepsilon,t) \tag{57}$$

divided by its thermal value is shown in Fig. 8. We display the ρ-integrated distribution function at three different times ($tn_e v_e b^2 = 0.1, 1$, and 10) as well as the time asymptotic result ($t = \infty$). We again focus your attention to the steady state values shown as diamonds. The ρ integration takes the average of the full distribution function shown in Fig. 7 along a horizontal line of constant ε. This allows us to display in a more quantitative way how quickly the distribution function is depleted by many orders of magnitude as one moves beyond the bottleneck.

Another interesting feature of Fig. 7(e) is illustrated by the average $\varepsilon\rho$ value

$$\langle \varepsilon\rho \rangle \equiv \frac{1}{W_{\rm ss}(\varepsilon)} \int_0^{1/\varepsilon} d\rho (\varepsilon\rho)\, W_{\rm ss}(\rho,\varepsilon), \tag{58}$$

which is plotted in Fig. 9. This graph shows that the value of the moment $\langle \varepsilon\rho \rangle$ is larger than the value for a thermal equilibrium distribution. This has a rather simple explanation. First, remember that collisions that do not involve an elec-

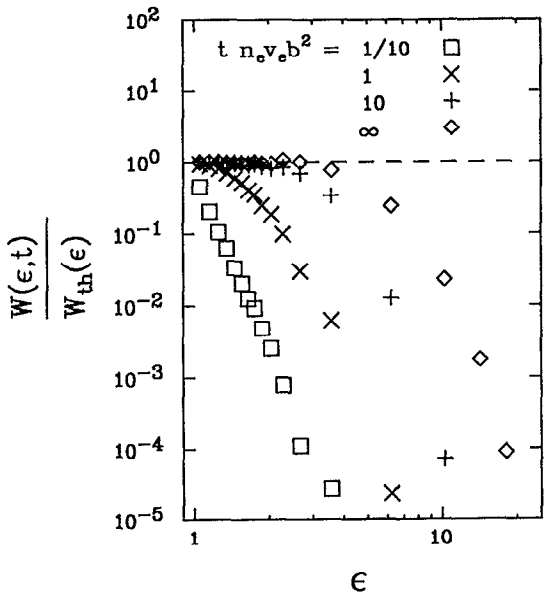

FIG. 8. The ρ-integrated distribution function at various times. The time marked ∞ corresponds to steady state. The dashed line is thermal equilibrium.

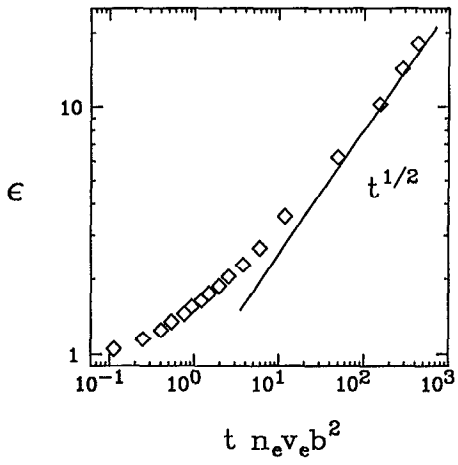

FIG. 10. Location of the front of occupation as a function of time. The time is when the ρ-integrated distribution function reaches 1/2 of its steady-state value.

tron exchange do not change ρ values. In $(\varepsilon\rho,\varepsilon)$ space this corresponds to remaining on the same line through the origin, $\varepsilon = (1/\rho)\varepsilon\rho$. To change the value of ρ [i.e., jump off the line, $\varepsilon = (1/\rho)\varepsilon\rho$] a collision involving an electron exchange must occur; but only a small fraction of the collisions, ($\sim\frac{1}{100}$) involve electron exchange. What happens is that below the bottleneck an atom hops along a line of constant ρ until an electron exchange collision occurs. Initially the atom will usually be formed at a large ρ value. It will then have to wait for the rare exchange collision to be able to jump to the lines with smaller ρ. This causes a traffic jam of atoms at large ρ since the routes to smaller ρ are partially blocked. The final result is that the distribution function is skewed toward larger ρ values, and this increases the moment $\langle\varepsilon\rho\rangle$ relative to the thermal equilibrium value.

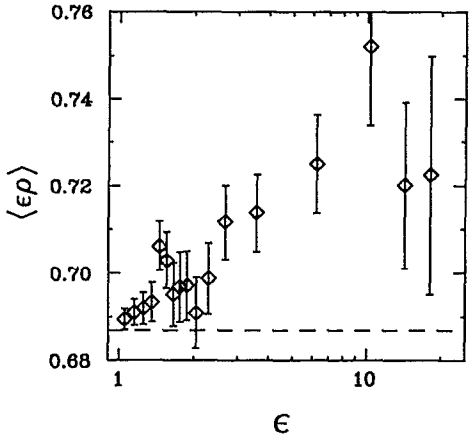

FIG. 9. The ρ-integrated moment $\langle\varepsilon\rho\rangle$ in steady state for different values of ε. The dashed line shows the value expected if the distribution is thermal.

We now turn our attention to the time dependence of the distribution function; that is, to the question of how fast the steady state is established. The evolution of the distribution function $W(\rho,\varepsilon,t)$ from its initial condition to its steady state is illustrated in Figs. 7 and 8. One can see a front of occupation that moves to deeper binding as time progresses.

The location of the front as a function of time [i.e., $\varepsilon = \varepsilon(t)$] is shown in Fig. 10. It is obtained by plotting the time for which the ρ-integrated distribution function reaches one-half of its steady-state value. This time is also characteristic of how long it takes a typical atom to cascade to a given energy ε. At large time, the location of the front scales as $\sqrt{t}$. This scaling can be explained by a simple argument. Assume that the rate of a collision of an electron with an atom R_a is proportional to the area within the cutoff radius $R_a \sim \rho_c^2$, where ρ_c is defined in Eq. (47). Note that for large ε, ρ_c scales as ε^{-1}. From an independent numerical calculation, the average step in energy $\langle\Delta\varepsilon\rangle$ is found to be proportional to ε for both electron exchange and nonexchange collisions, that is $\langle\Delta\varepsilon\rangle \sim \varepsilon$. For energies below the bottleneck we make the further assumption that the atom must step in energy toward deeper binding during the course of each collision until it reaches the sink. To populate a certain energy level we must wait long enough for the average atom to reach that level, so the rate at which the front moves is determined by

$$\frac{d\varepsilon}{dt} = R_a \langle\Delta\varepsilon\rangle \sim \varepsilon^{-1}, \tag{59}$$

which has the solution $\varepsilon(t) \sim \sqrt{t}$. The prediction of this simple argument is that the location of the front should scale as $\sqrt{t}$ for large binding energies—a prediction the data supports.

To show the relationship between the Monte Carlo simulation and the analytic work, a set of runs are done using different values of $\varepsilon_{\rm th}$. Only the one-way rate of $\varepsilon_{\rm th}$ crossing $R_\uparrow(\varepsilon_{\rm th})$ is measured. The results are shown in Fig. 11. Also plotted is the numerical evaluation of the flux integral Eq. (41) for three values of the free parameter C, the adiabatic

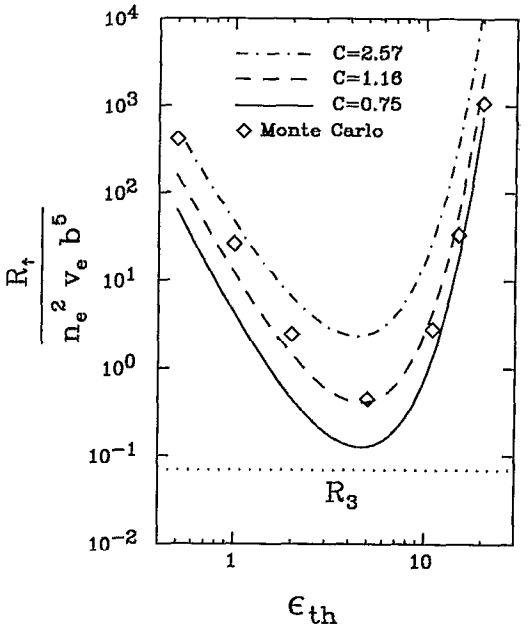

FIG. 11. One-way rate of crossing a surface of constant energy if the system is in thermal equilibrium. Shown is the Monte Carlo calculation of this rate (◇) and the analytic estimate Eq. (41) of this rate for three values of the adiabatic cutoff C. Also shown is the Monte Carlo estimate of the recombination rate R_3.

cutoff. The rate $R_\tau(\varepsilon_{\rm th})$ can be compared to the one-way flux expressed analytically in Eq. (41). Recall that the analytic calculation of the one-way flux may count a collision multiple times because of recrossings of the surface $\varepsilon = \varepsilon_{\rm th}$ during the course of one collision. We introduced the adiabatic cutoff C to compensate for this effect. The Monte Carlo rate $R_\tau(\varepsilon_{\rm th})$ does not have this problem since it only considers the state before and after a collision, that is, $R_\tau(\varepsilon_{\rm th})$ is the one-way flux corrected for recrossings. A comparison of the two results determines the value C which would compensate for recrossings. From Fig. 11 one can see that the minimum $R_\tau(\varepsilon_{\rm th})$ at $\varepsilon_{\rm th} = 5$ corresponds to an adiabatic cutoff of $C = 1.2$. Also shown in Fig. 11 is the recombination rate determined by the Monte Carlo simulation R_3 which is a factor of 6 less than the minimum value of $R_\tau(\varepsilon_{\rm th})$. This difference is caused by the finite width of the bottleneck and the skewing of the distribution function toward larger ρ values.

VI. CONCLUSIONS AND DISCUSSION

By using a Monte Carlo simulation, we have calculated the three-body recombination time R_3^{-1} for ions that are introduced into a cryogenic and strongly magnetized pure electron plasma. The rate given by $R_3 = 0.070(10) n_e^2 v_e b^5$ is an order of magnitude smaller than the rate obtained previously for an unmagnetized plasma. Also determined by the simulation is the characteristic time for an electron–ion pair to cascade to a given level of binding. For deep binding,; this time is given by Fig. 10 to be of order an evolution time $(n_e v_e b^2)^{-1}$ multiplied by ε^2.

It is instructive to discuss these two quantities in terms of a simple physical example. Consider a cryogenic pure electron plasma that is confined in a Penning trap; the plasma has the shape of a long column (say, of length L) with the radial confinement provided by an axial magnetic field and the axial confinement by electrostatic fields applied at each end. Suppose that an ion transits the full length of the plasma, drifting with a small velocity $v_{i\|}$ along the magnetic field. If the transit time is long compared to the recombination time (i.e., $R_3 L / v_{i\|} \gg 1$), the ion recombines with nearly 100% probability, and the electron–ion pair is deeply bound when it exists the plasma. If the transit time is long compared to the evolution time but small compared to the recombination time, the probability of recombination during transit is given by $R_3 L / v_{i\|}$. For a typical recombined pair, the depth of binding is given by the plot of $\varepsilon(t)$ in Fig. 10, where the time is to be interpreted as $t = (L / v_{i\|})$. It is important that the binding be deep enough to avoid ionization by the electrostatic confinement field at the end of the trap. (The external field should be small compared to the binding field.) If the transit time is short compared to the evolution time, the calculated recombination rate (steady-state flux to the sink) is not applicable. For this case, it is very unlikely that a recombined pair would survive the electric field at the end of the plasma.

Next, let us reexamine the approximations used in the theory. The guiding center approximation breaks down at sufficiently deep binding [i.e., $\varepsilon \gtrsim (b / r_{ce})^{2/3}$] and all three degrees of freedom begin to interact on an equal footing. The motion becomes chaotic, and the perpendicular kinetic energy (that had been tied up in the cyclotron adiabatic invariant) is shared with the other degrees of freedom. One might worry that this would lead to ionization, but it cannot since the perpendicular kinetic energy is of order $k_B T_e$ and the binding energy is much larger than $k_B T_e$. Of course this assumes that the guiding center approximation does not break down until the binding energy is well below the bottleneck. Also, the one-way flux to deeper binding below the bottleneck is not changed qualitatively by the breakdown of the guiding center approximation. The nature of the bottleneck and of the flux is determined by a competition between the Boltzmann factor and a phase space factor, and this competition is modified only slightly (by one power of ε in the phase space factor) when all degrees of freedom are involved.

At sufficiently deep binding, classical mechanics no longer provides an adequate description of the dynamics, and one might worry that quantum effects (e.g., metastable states) would modify the evolution rate. In this paper, quantum effects have not been considered at all; we assume that the classical description is valid down to binding energies such that the bound pair can survive the electrostatic confinement field at the end of the trap.

Finally, the analysis treats the ions as stationary. The ion motion parallel to the magnetic field is negligible compared to the electron motion provided that $v_{i\|} \ll v_e$. The condition that the perpendicular motion be negligible is more restrictive. For an electron–ion pair that is separated by the distance $r = |\mathbf{r}_e - \mathbf{r}_i|$, the frequency of the $\mathbf{E}\times\mathbf{B}$ drift mo-

tion of the electron around the ion is $\omega_{\mathbf{E}\times\mathbf{B}} = ce/Br^3$. The transverse ion motion is characterized by two frequencies Ω_{ci} and $v_{i\perp}/r$; so the condition that the ion motion be slow compared to the electron motion is $v_{i\perp}/r, \Omega_{ci} \ll ce/Br^3$. In these inequalities, the electron–ion separation may be replaced by b, since we follow the dynamics only for binding energies $\varepsilon > \varepsilon_{\rm th} \cong 1$. The rest of phase space (i.e., $\varepsilon < \varepsilon_{\rm th}$, which corresponds to $r > b$) is characterized by a thermal equilibrium electron distribution and we do not care if the ion motion is negligible or not. By using $r \approx b = e^2/mv_e^2$ the inequalities can be rewritten as $v_{i\perp} \ll (r_{ce}/b)v_e$ and $1 \ll (m_i/m_e)(r_{ce}/b)^2$.

When the latter of these two inequalities is reversed, the ion cyclotron frequency is larger than the $\mathbf{E}\times\mathbf{B}$ drift frequency. In this case, the electron and ion $\mathbf{E}\times\mathbf{B}$ drift together across the magnetic field with the velocity $v_{\mathbf{E}\times\mathbf{B}} \cong ce/Bb^2 = v_e(r_{ce}/b)$. The results of our calculation should still apply since the drifting pair maintain a constant separation. It does not matter to the cascade process whether the electron is $\mathbf{E}\times\mathbf{B}$ drifting around a fixed ion at constant separation or the electron and ion are drifting together at constant separation.

When the first of the two inequalities is reversed, the ion can run away from the electron before the electron completes an $\mathbf{E}\times\mathbf{B}$ drift circuit around the ion. In this case, one expects a substantial reduction in the recombination rate. A simple dimensional argument suggests a rate of order $R_3 \sim n_e^2 v_e r_0^5$, which is a reduction by the factor $(r_0/b)^5$, where r_0 is the electron–ion separation for which the $\mathbf{E}\times\mathbf{B}$ drift velocity equals the perpendicular ion velocity (i.e., $v_{i\perp} = ce/Br_0^2$). A detailed analysis of the recombination rate for the case where ion motion is included will be presented in a future paper.

ACKNOWLEDGMENTS

This work was supported by a National Science Foundation Graduate Fellowship, the San Diego Supercomputer Center, and National Science Foundation Grant No. PHY87-06358.

[1] J. H. Malmberg, T. M. O'Neil, A. W. Hyatt, and C. F. Driscoll, in *Proceedings of 1984 Sendai Symposium on Plasma Nonlinear Phenomena* (Tohoku U. P., Sendai, Japan, 1984), pp. 31–37.

[2] D. R. Bates, Adv. At. Mol. Phys. **20**, 1 (1985).

[3] G. Gabrielse, S. L. Rolston, L. Haarsma, and W. Kells, Phys. Lett. A **129**, 38 (1988).

[4] D. R. Bates and A. Dalgarno, *Atomic and Molecular Processes* (Academic, New York, 1962), p. 245.

[5] G. Gabrielse, Hyperfine Interactions **44**, 349 (1988).

[6] C. M. Surko, M. Leventhal, and A. Passner, Phys. Rev. Lett. **62**, 901 (1989).

[7] G. Gabrielse, X. Fei, K. Helmerson, S. L. Rolston, R. T. Tjoelker, T. A. Trainor, H. Kalinowsky, J. Hass, and W. Kells, Phys. Rev. Lett. **57**, 2504 (1986); G. Gabrielse, X. Fei, L. A. Orozco, R. L. Tjoelker, J. Haas, H. Kalinowsky, T. A. Trainor, and W. Kells, *ibid.* **63**, 1360 (1989).

[8] P. Mansback and J. C. Keck, Phys. Rev. **181**, 275 (1969).

[9] D. R. Bates and I. Mendas, J. Phys B **8**, 1770 (1975).

[10] B. Makin and J. C. Keck, Phys. Rev. Lett. **11**, 281 (1963).

[11] R. G. Littlejohn, Phys. Fluids **24**, 1730 (1981).

[12] T. G. Northrop, *The Adiabatic Motion of Charged Particles* (Interscience, New York, 1963).

[13] G. E. Uhlenbeck and G. W. Ford, *Lectures in Statistical Mechanics* (American Mathematical Society, Providence, RI, 1963).

[14] E. M. Lifshitz and L. P. Pitaevskii, *Physical Kinetics* (Pergamon, Oxford, 1981).

[15] J. C. Keck, Adv. Chem. Phys. **13**, 85 (1967).

[16] N. G. Van Kampen, *Stochastic Processes in Physics and Chemistry* (North-Holland, New York, 1981).

[17] N. A. Krall and A. W. Trivelpiece, *Principles of Plasma Physics* (San Francisco Press, San Francisco, 1986).